Air intrusion on pipe-filling bores in quasi-horizontal pipelines

Report UMCEE-04-01

Jose G. Vasconcelos
and
Steven J. Wright

Department of Civil and Environmental Engineering
The University of Michigan
College of Engineering

Ann Arbor, MI 48109-2125

Air intrusion on pipe-filling bores in quasi-horizontal pipelines

Report UMCEE-04-01

Jose G. Vasconcelos
and
Steven J. Wright

University of Michigan
Department of Civil and Environmental Engineering
Ann Arbor, Michigan

April 7, 2004

Summary

The construction of below-grade storage tunnels is one alternative to attenuate the adverse impacts of storm runoff discharge in water bodies. These tunnels are usually design to operate in a free-surface flow regime, but intense rain events significantly alter the system behavior. Briefly, these changes are: development of moving bores; flow regime transition into pressurized flow; and potential pressurization of the air phase within the tunnel. Past research promoted at the University of Michigan focused on the effects of air phase pressurization (Vasconcelos and Wright, 2004a). In that study it was determined that under certain circunstances the pipe-filling bore that causes the flow regime transition experiences an air intrusion on its top. This intrusion, referred as "interface breakdown" abbreviated as IBD, eventually evolves into an air pocket that remains trapped in the system. The importance of this occurrence comes from the operational problems such air pockets cause to the storage tunnels when they are suddenly expelled through venting points. This report aims to detail the conditions in which IBD occurs by means of experimental investigations promoted on a 1:50 scale model. A single-phase numerical model is used to predict the occurrence of the relevant flow features. Results indicate that the IBD is directly related to the effects of the air pressurization on the free-surface portion of the flow during the rapid filling event, and that one dimensional numerical models are capable of predict such occurrences.

Contents

Chapter 1

Historical Perspective and Motivation

1.1 The rapid filling pipe problem in stormwater sewers

The changes in the land use caused by urbanization have resulted in several adverse impacts to watersheds. One of the impacts is the degradation of the water quality of storm run-off, which causes the disruption of many environmental processes in receiving water bodies (Zoppou, 1999). Another adverse impact is the increased run-off peak flow and the greater amount of run-off volume, which can result in erosion in the receiving water body.

Among the different alternatives to minimize these problems, one is the construction of below-grade stormwater storage tunnels. These tunnels provide storage capacity to attenuate peak flow discharge, and they may provide treatment to improve the stormwater quality before the environmental release, such as sedimentation and chlorination. They are preferred over other catchment alternatives particularly in densely occupied areas where the price of land acquisition is too high.

These tunnels are designed to operate in free-surface flow regime, but according to the literature (Guo and Song, 1990, 1991; Zhou et al., 2002) the flow regime may change into pressurized flow during intense rain events. As a consequence of this pressurization process, serious operational problems in these tunnels may occur, including geysering through manholes and other vertical shafts and structural damages due to waterhammer-like pressures. This occurrence is also referred in the literature as flow regime transition.

The hydraulics of these tunnels are significantly altered during intense rain events. During the initial stages, upon increase of the inflow, there will be the formation of a flood wave that will propagate within this tunnel. That flood wave in turn may evolve into a moving hydraulic jump (bore) depending on the dimensions and the characteristics of the flow. After some reflections at the system boundaries, a pipe-filling bore will eventually develop separating the free-surface flow ahead of the bore and the pressurized flow behind the bore.

During regular rain events, the incoming water flow usually expels the air phase present in the tunnels causing no air pressurization, but that can be changed during intense rain events. As long as the available ventilation is adequate, the air phase would be evacuated without become pressurized, and that in turn wouldn't cause changes to the system dynamics. However, depending on geometry characteristics and inflow conditions, the available ventilation may be reduced, resulting in possible pressurization of the air phase. In such cases, the air phase needs to be incorporated in the analysis.

The rapid filling pipe problem and the flow regime transition applied to tunnels has been studied for many decades. Experimental investigations date since 1932, pioneered by Meyer-Peter and

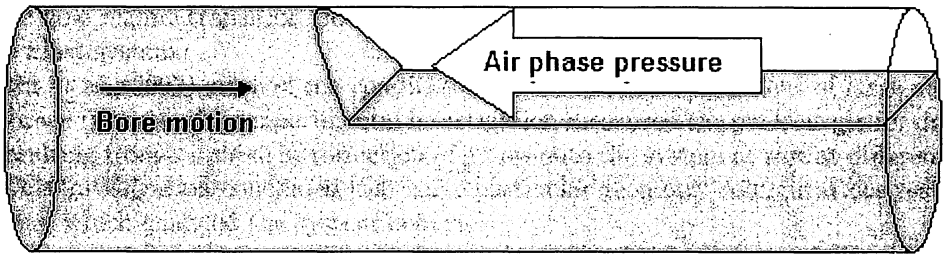

Figure 1.1: Air cushioning effect on the pipe filling bore

Favre in their study of the Wettingen powerplant outlet tunnel (Hager, 2001). Subsequent investigations focused mainly on the numerical predictions of the flow regime transition, as exemplified by the works by Wiggert (1972), Cunge et al. (1980), Song et al. (1983). Those works, however, don't include the air phase in the calculations, assuming implicitly that the air phase has enough ventilation. The following section presents a review of the studies that include the air phase in their analysis of this problem.

1.2 Research on air phase effects in stormwater systems undergoing rapid filling

There have been investigations that include the effects of the air phase in the rapid filling pipe problem, and one of the first studies in this direction was presented by Hamam and McCorquodale (1982). The authors propose a numerical model that accounts for the air pressurization in the flow regime transition reducing the bore speed propagation, as indicated in figure 1.1. There was no indication on how to calculate the air phase pressure. This work was later improved by Li and McCorquodale (1999) by including a method to obtain the air phase pressure and by allowing for the formation and motion of air pockets caused by shear force instabilities between the air and water phases. This feature is very interesting since these pockets are can play a important role in causing operational problems such as geysering or waterhammer pressures.

Nguyen (1999) proposed a numerical model to simulate the flow in a conduit in the presence of an air cushion. This approach is an improvement in the sense that the effects of air pressurization aren't limited to the bore propagation. This single-phase model includes the air phase pressure in the momentum equation of the water phase. The model is able to predict the motion of the free surface portion of the flow generated by the air pressure gradient. Yet, there's no adequate treatment for the fate of the air phase pressure after the volume of the air within the system goes to a minimum. No experimental investigation was conducted to confirm the results obtained with the model.

Zhou et al. (2002) studied the problem of the water advance through an initially empty pipe assuming that a vertical interface represented the pipe filling bore. This study aims to characterize the different types of pressure peaks a system would experimence with different degrees of ventilation, and both experiments and a numerical model were developed. However, the assumption of a

vertical interface as the pressurization bore may not be so adequate to represent actual systems, in which the flow regime transition would be in the form of a moving pipe-filling bore advancing in a partially filled system.

Wright et al. (2003) studied the conditions related to the development of large surges in below grade storage tunnels. This experimental investigation measured the peak surges for different tunnel slopes resulting from a sudden introduction of inflow onto the system at rest at different initial water levels. This investigation concluded that some particular geometry configurations result in trapped air pockets, which changed the system behavior.

Further experimental investigations were promoted by Vasconcelos and Wright (2004a) to determine the type of interactions between air and water phases during the rapid filling pipe event. One outcome from these investigations was the confirmation that the air pressurization effects are not limited to the pressurization bore alone, but can be felt throughout the system. It was shown that the possible interactions between air and water phases in downward sloped tunnels is controlled basically by the amount of ventilation provided in the system. These interactions can be summarized as follows:

1. When the initial water level of the system is low, then ventilation will be adequate and no signs of air pressurization will be noticed;

2. As the initial water level increases above some level, then it will be possible to notice the motion of the water in the free-surface portion of the system towards the surge tank. That flow feature was referred as "pre-bore motion" or PBM, as seen in figure 1.2;

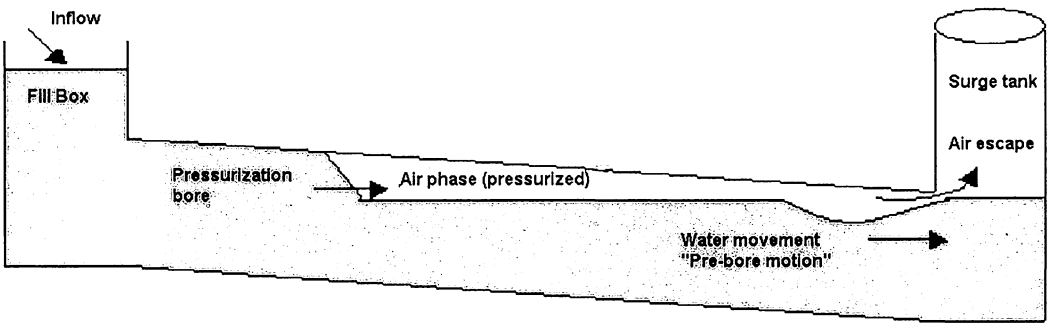

Figure 1.2: Scheme of the occurrence of the "pre-bore motion" feature. Vertical scale is exaggerated

3. Further increase of the initial water level will lead to a condition when the pipe-filling bore will experience an upstream intrusion of air at the top (see figure 1.3). Following the occurence of this intrusion, the bore will resume the movement towards the surge tank, but not closing the entire cross section. The air pocket will move upstream in a shape resembling a gravity current. That feature was referred as "interface breakdown", or IBD;

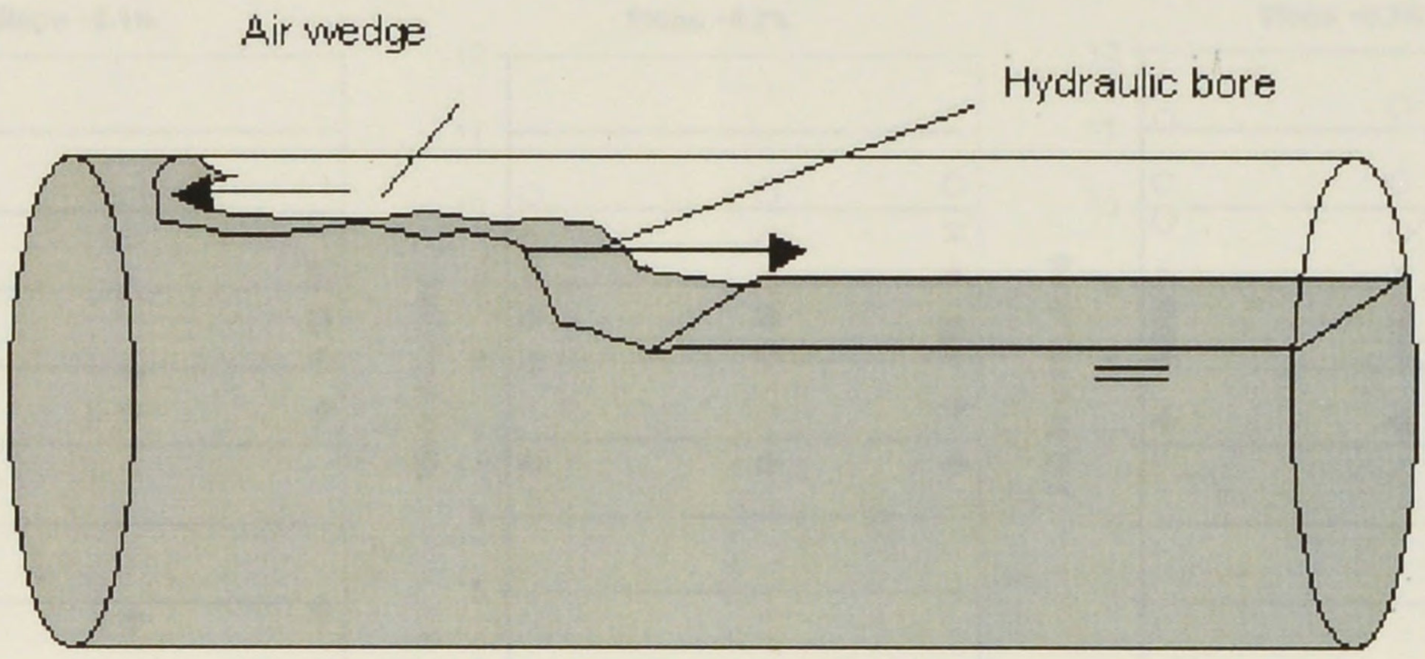

Figure 1.3: Scheme of the occurrence of the "interface breakdown" feature

4. If initial water level is increased even more, the formation of a pipe-filling bore does not occur, but rather an undular bore propagates downstream. Air pressurization seems to occurs rapidly, and an expulsion of air through the upstream end was observed almost immediately. It was shown that if adequate venting conditions were provided, the undular front was replaced by a pipe filling bore. Generally, undular bores did not completely fill the pipe cross section. A schematic of this flow condition is shown in figure 1.4;

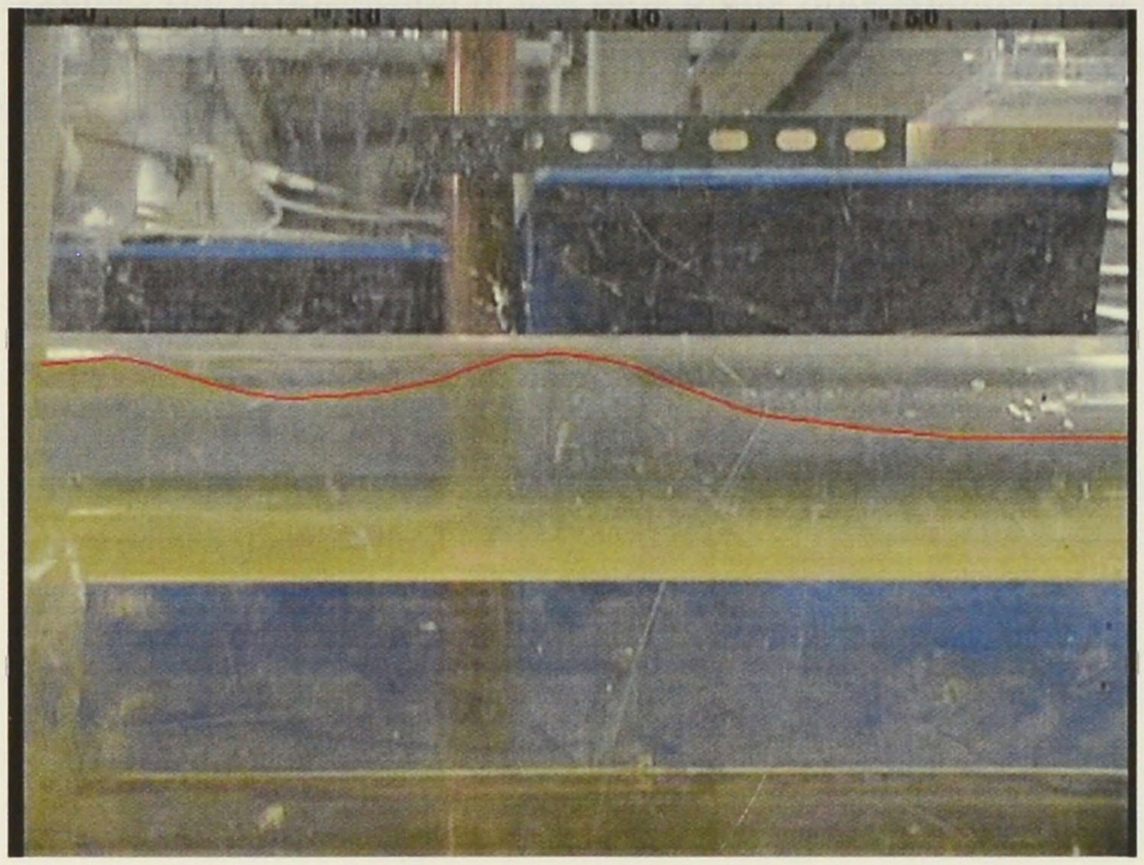

Figure 1.4: Scheme of undular front propagation

The results with this investigations are summarized in the graph presented in figure 1.5.

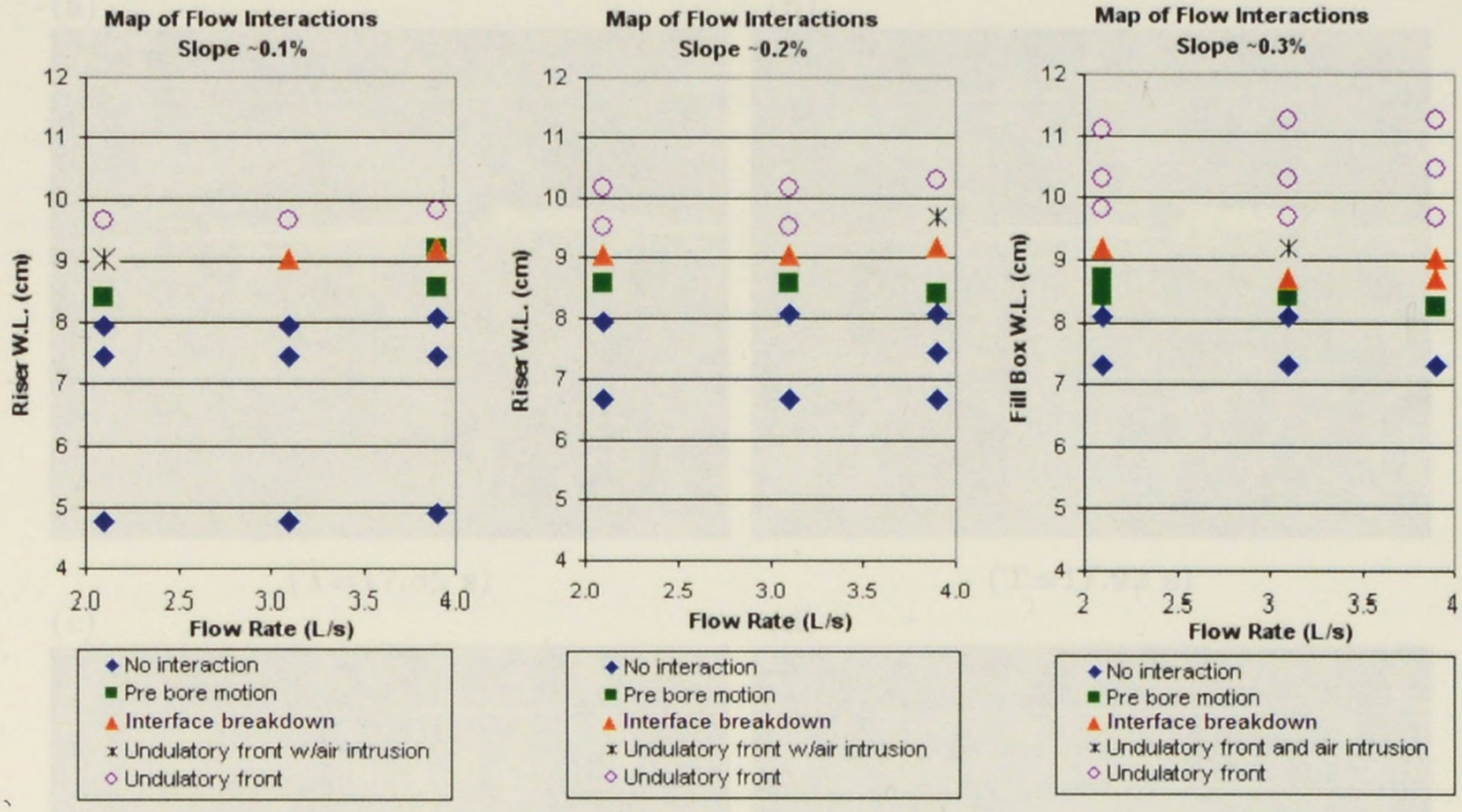

Figure 1.5: Map of flow interactions during rapid filling events (Vasconcelos and Wright, 2004a)

Figure 1.6 details the occurrence of a IBD event with four snapshots taken with a digital camcorder. Snapshot (a) shows the propagation of the pipe filling bore coming from the right. Snapshot (b) shows the IBD onset at the top of the pipe. Snapshots (c) and (d) show the enlargement of the air intrusion as the bore moves downstream.

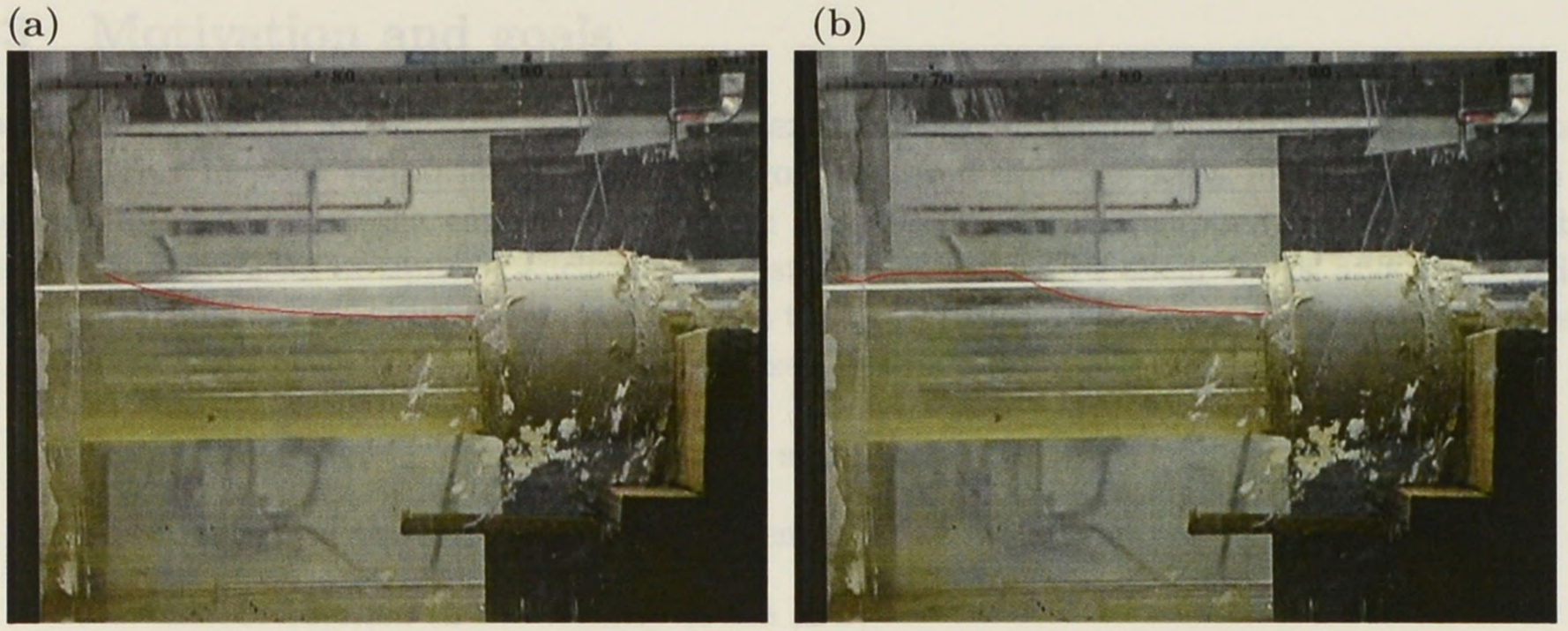

Figure 1.6: Four snapshots detailing one IBD event. The upper scale units are in 10 cm

Subsequent attempts to model numerically these interactions (Vasconcelos and Wright, 2004b) were successful in describing the occurrence of "pre-bore motion". The models were able to predict the air cushioning effect of the air phase, and also the changes to the system behavior caused by PBM, including the changes on the bore speed caused by this flow feature. This study pointed to the difficulties and limitations of model approaches in cases when IBD occurred. Nevertheless, it is important to understand the flow conditions related to the occurrence of "interface breakdown" since it results in air pocket formation, which is one major source of operational problems in storage tunnels.

1.3 Motivation and goals

This report aims to present the results of the experimental investigations on the IBD phenomena occurring in poor ventilated tunnels undergoing a rapid filling process. The motivation is to understand and predict the conditions in which air pockets may be trapped due to IBD. Other sources of air pockets in tunnels, such as flow instabilities caused by shear forces and propagation of undular fronts are also important, but it is not the objective of the present work to discuss them. In summary, the following list of topics is discussed in this report:

- Description of the experimental apparatus and procedure;
- Determination of the limits of IBD occurrence;
- Flow characterization in the vicinity of the IBD;
- Tentative approach to predict the occurrence of IBD.

Chapter 2

Experimental description

2.1 Experimental apparatus

This chapter presents the experimental settings and procedures used in the investigations to determine the conditions in which the "interface breakdown" phenomena occurs.

The experiments studying IBD modified the experimental apparatus originally used by Wright et al. (2003) to study the conditions in which large surges would develop in below grade storage tunnels. The apparatus is a scale model that was constructed based on a proposed flow-through tunnel and storage system for the city of Dearborn, Michigan. A detailed account of the model conception is provided in that work. The resulting model scale is roughly 1:50, with a model length of 14.6 m and a diameter of approximately 9.4 cm. Clear acrylic tubing was used in the model construction in order to observe the movement of bores and trapped air within the tunnel.

In actual storage tunnels, the inflow is controlled by rainfall/runoff process, resulting in a time-variable inflow that can hardly be replicated in laboratory conditions. Some simplifications with regards to the inflow hydrograph were then required, and can be summarized as follows. It was decided to simply input water at a constant flow rate representing the peak discharge on the inflow hydrograph. To account for the volume accumulated in the initial stages of the rising hydrograph, the inflow was initiated with the pipe partially filled. Therefore, the simplified representation of the inflow hydrograph was based on different values of inflow rates and initial water levels.

A overhead pipe with a two-way valve provided flow to the scale model. This inflow was admitted through a storage box of limited height, which modeled the overflow elevation at the downstream end of each tunnel segment of the proposed system. When the storage capacity of the model was exceeded the inflow box also operated as overflow point. This arrangement was conceived to maximize the chances of a pipe-filling bore, since if the flow was introduced in an intermediary point two smaller bores would be generated instead upon flow initiation. The experimental measurements were promoted during the transition between two different steady conditions: the initially stagnant condition, and the condition when the inflow at the fill box matches the outflow spilling over the crest of that box.

The fill box had a rectangular cross-section of 0.25 m by 0.25 m, and an adjustable spill level, with maximum level approximately 0.216 m above the pipe crown. For the maximum spill level, the crest of the fill box essentially behaved as a sharp-crested weir. For lower spill levels, only the back face of the fill box operated as a sharp-crested weir. Steady state measurements were made to determine the head in the fill box as a function of the overflow rate for each spill level considered.

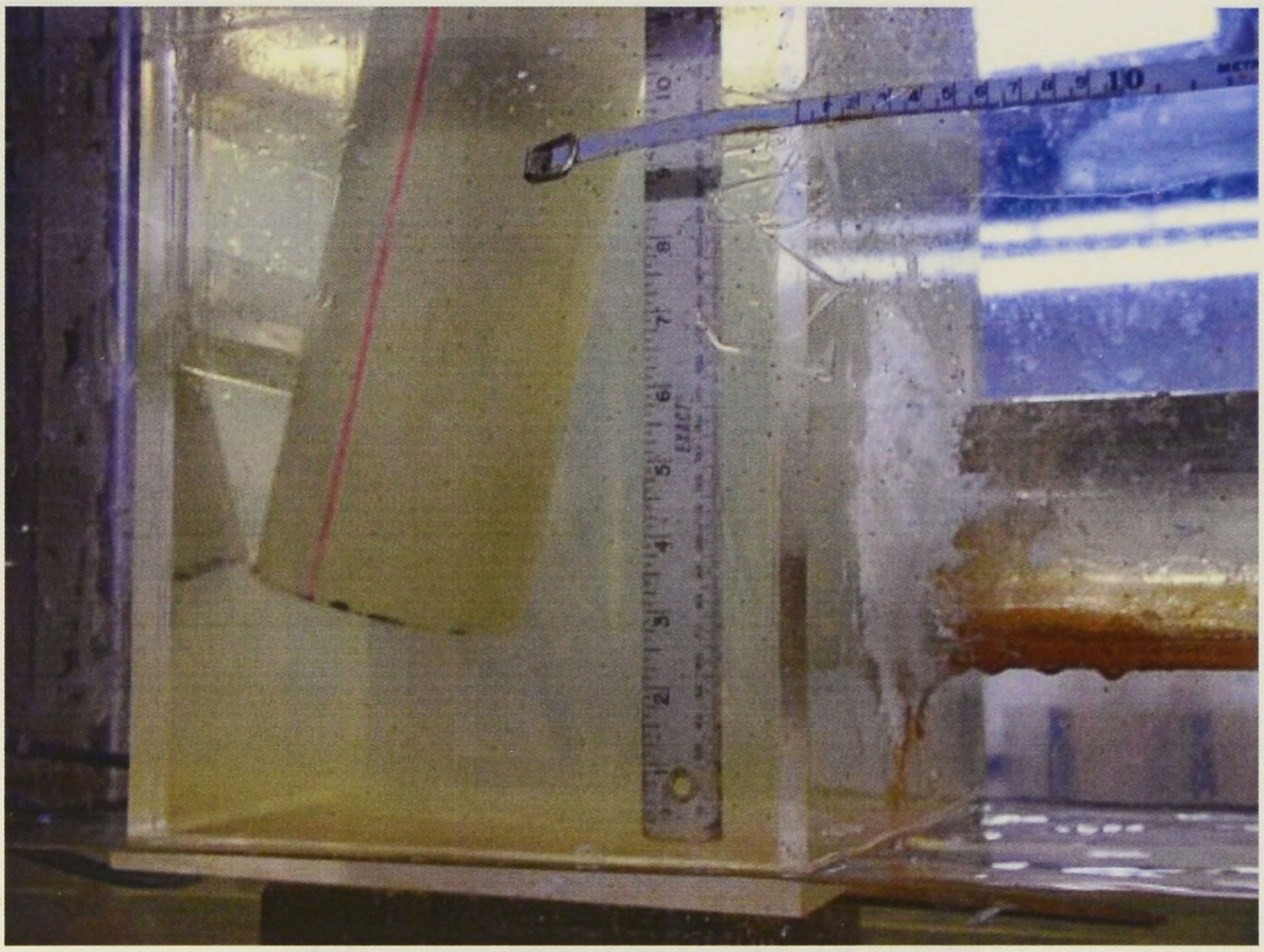

Figure 2.1: Photograph of the fill box used in the experiments

For all experiments, it was defined that the reference depth would be the depth measured at the fill box. Figure 2.1 shows a photograph of the fill box used in the experiments.

In the original scale model there was a chamber at the end of the pipe that modeled the behavior of the surge chamber in the proposed storage tunnel design. It was comprised of a vertical surge tank (also referred as riser) , with circular cross-section with 0.19 m diameter. The height of this tank is much greater than the overflow level of the fill box, which resulted in the confinement of the surges observed during the experimental runs. Figure 2.2 shows a photograph of the surge tank used in the experiments.

Changes were made in the ventilation arrangements of the physical model in order to simplify the air discharge. At the upstream end, the fill box, the initial conditions of depth and inflow rates should be such that a pipe-filling bore would form rapidly upon flow admission in the system. At the surge tank the air ventilation was closed with the help of a barrier which projected below the water surface, effectively blocking the air communication between the pipe and the surge tank. Finally at the surge tank end a venting tower was opened, in which a 1/4" diameter rounded nozzle was placed to control the rate at which air could escape through the vent tower. Previous experiments indicated that this nozzle size resulted in IBD formation. A schematics of the resulting system is presented in figure 2.3.

Figure 2.2: Photograph of the surge tank used in the experiments

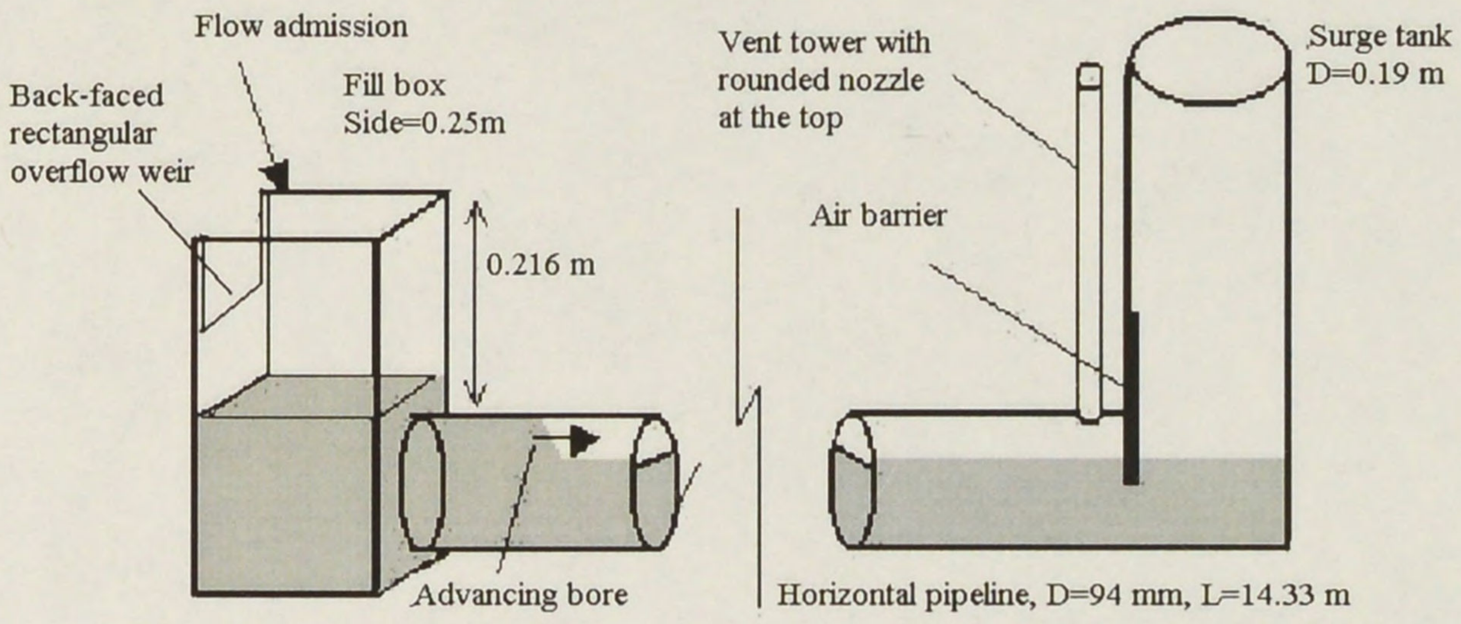

Figure 2.3: Scheme of the physical model used on for model comparison

2.2 Experimental procedure

In general, the experimental procedure for all the experiments was the following:

1. Set a initial water level in the system and let it repose until no surface waves can be observed;
2. With the two-way valve adjusted to discharge outside the tunnel, the desired flow was initiated and allowed to achieve steady conditions;
3. The two-way valve was then rapidly switched so the flow was admitted into the fill box;
4. The resulting undulatory/bore front was followed and qualitative observations with regards to the interactions between air and water phases were promoted. Depending on the specific goal of the experiment, different measurements were promoted. The measurements are detailed in the following chapters.

The list of measurement devices used in the IBD experiments is the following:

- Three piezoresistive pressure transducers, manufactured by Endevco, model 8510B-1 (1 PSIg);
- Data acquisition board, manufactured by National Instruments, model DAQ-Pad MIO-16XE-50;
- Acoustic doppler velocimeter (ADV), manufactured by Sontek;
- Digital camcorder with 30 frames per second speed;
- VHS camcorder.

The following chapters discuss the sequence of experiments promoted and their results.

Chapter 3

Delimiting IBD occurrence

Phase one of the IBD experiments addressed the fundamental question of what are the flow conditions in which air intrusion on the pressurization bores would occur. To address this question, a systematic study was conducted to assess the effect of basic parameters such as initial water depth, inflow rate and system geometry in the IBD occurrence.

An important issue was whether IBD could be triggered by events occurring at the system boundaries associated with the air phase pressurization. The significant events on the system boundaries during the filling process were two: when the upstream fill box starts spilling and when the surge level achieves an stable level. The rationale behind the importance of these events is based on the idea that what maintains the integrity of the pipe-filling bore would be a equilibrium condition that requires the upstream side of the bore to have higher pressure than the downstream side of the bore. Since the spilling of the fill box effectively results in an upper limit for the upstream pressure, the speculation was that this limit would affect the pressurization bore, causing the IBD occurrence. As for the surge tank level stabilization, it was assumed that once the level stabilized that would signal a "pressure equilibrium" condition, in which would pressures on both sides of the bores would be approximately equal.

It was considered that the key geometrical parameter was the spill level on the fill box, because that would ultimately control the time in which the above events would occur. Table 3.1 show the considered parameters and the range in which they were tested. As previously explained, the spill level at the fill box was set by adjusting the height of a sharp crested weir located at the back of the box. When the highest spilling level was used, all the sidewalls of the fill box had the same spilling level.

Table 3.1: System variables considered for IBD experiments - Phase one

Experiment variable	Range tested
Initial water depth (cm)	values around 6.0, 6.5, 7.0 and 7.5
Flow rate (L/s)	3.1 and 3.9
Spill level at fill box (cm)	18.8, 23.8 26.3 and 31.3

The combination of the conditions displayed in table 3.1 resulted in 32 experimental conditions. The following sections detail the findings grouped by the spill level in the system. In each of the experimental settings the inflow bore was followed to determine whether it would develop into a

pipe-filling bore and whether IBD would form.

The digital and VHS camcorders were placed on the surge tank and the fill box respectively, and the water level behavior was plotted against time. In those plots, the big diamonds indicate the moment when the IBD occurs according with each recorded movie. Because of the low precision of the VHS movie, in cases when there was discrepancies with regards to the timing of the IBD occurrence, the data provided by the digital camera was regarded as the more accurate.

3.1 Results for the 18.8 cm spill level

The results for the experimental settings using the 18.8 cm spill level are presented in figure 3.1 and in table 3.2.

Table 3.2: Results of IBD occurrence for the 18.8 cm spill level

Run	Inflow rate	Initial WL	IBD (Y/N)	Remarks/IBD location
A	3.1 L/s	6.0 cm	No	Undular front propagation
B	3.1 L/s	6.4 cm	No	Undular front propagation
C	3.1 L/s	7.0 cm	Yes	8.1 +/- 0.3 m from fill box
D	3.1 L/s	7.5 cm	Yes	9.0 +/- 0.3 m
E	3.9 L/s	6.1 cm	No	Undular front propagation
F	3.9 L/s	6.5 cm	Yes	8.1 +/- 0.3 m
G	3.9 L/s	7.0 cm	Yes	8.4 +/- 0.3 m
H	3.9 L/s	7.5 cm	Yes	9.3 +/- 0.3 m

The results in table 3.2 suggests that IBD occurrence is associated with higher initial water levels and inflow rates. For smaller initial water levels and inflows, the inflow was insufficient to form a pipe-filling bore, and consequently the development of IBD is unclear. In some of the settings with undular fronts, small air pockets were observed behind the undular bore. A tendency of IBD was also observed to occur further away from the fill box for higher initial water levels.

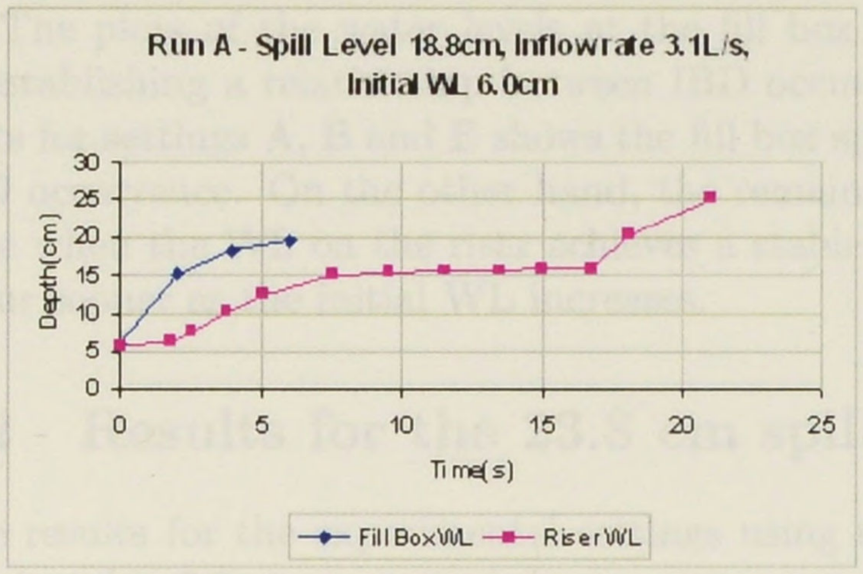

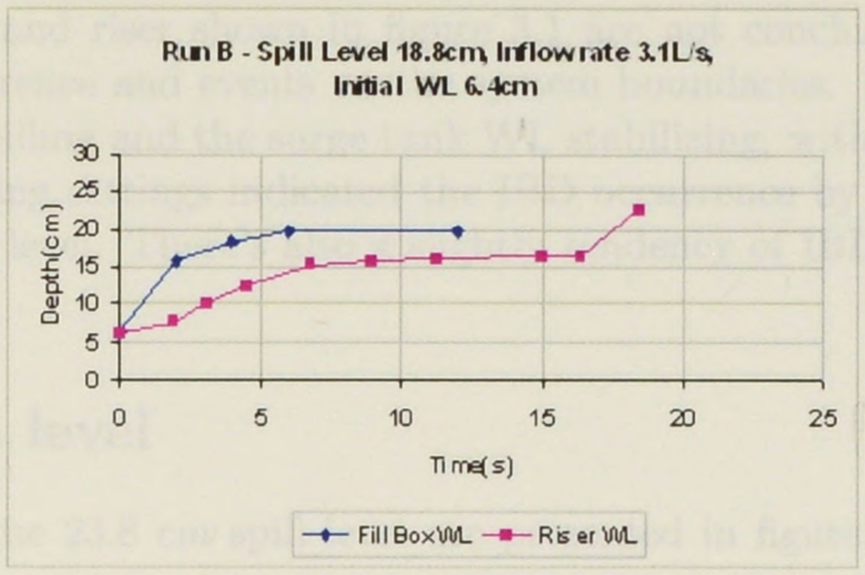

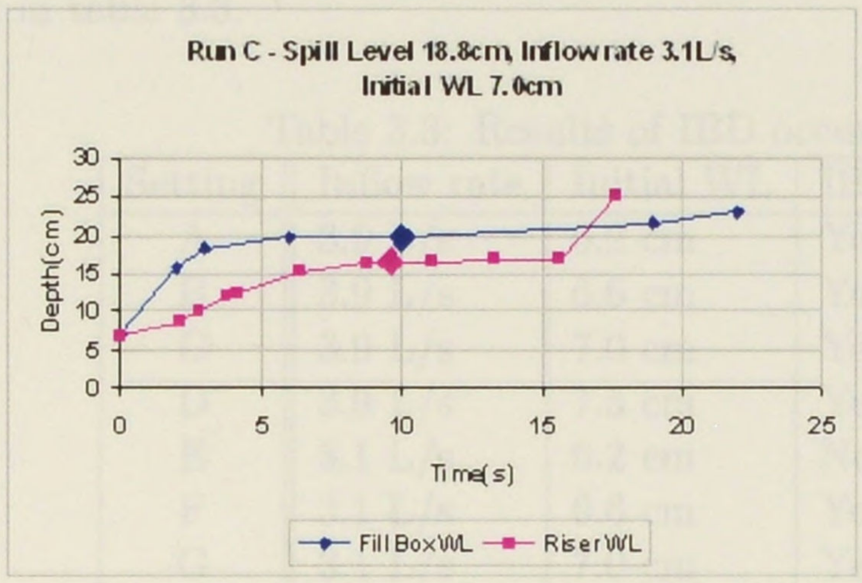

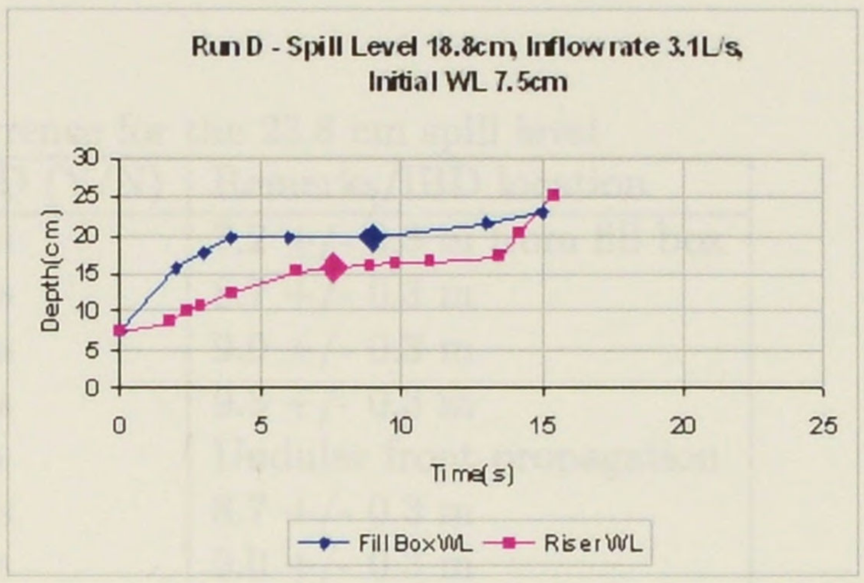

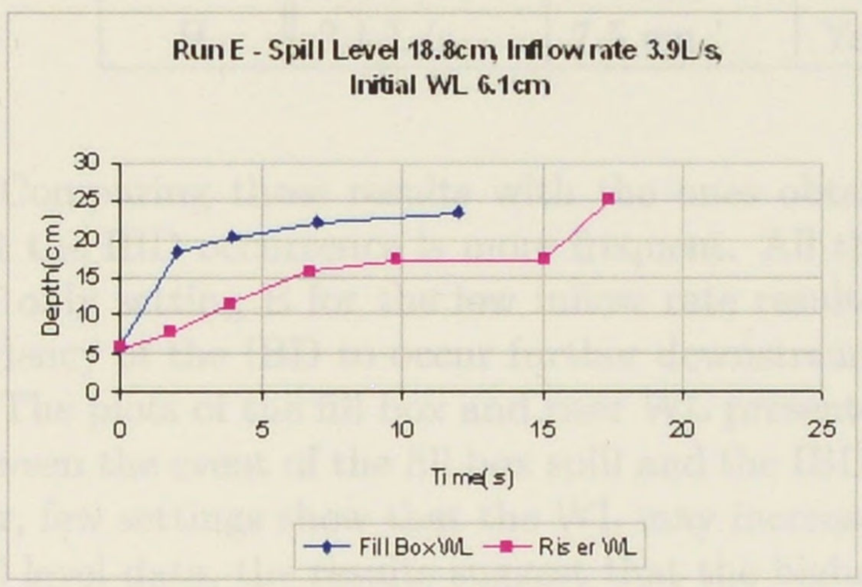

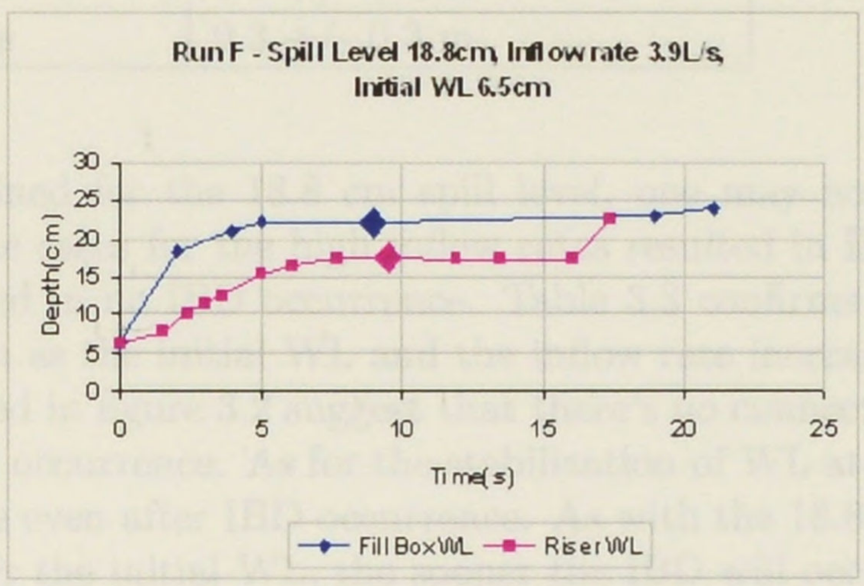

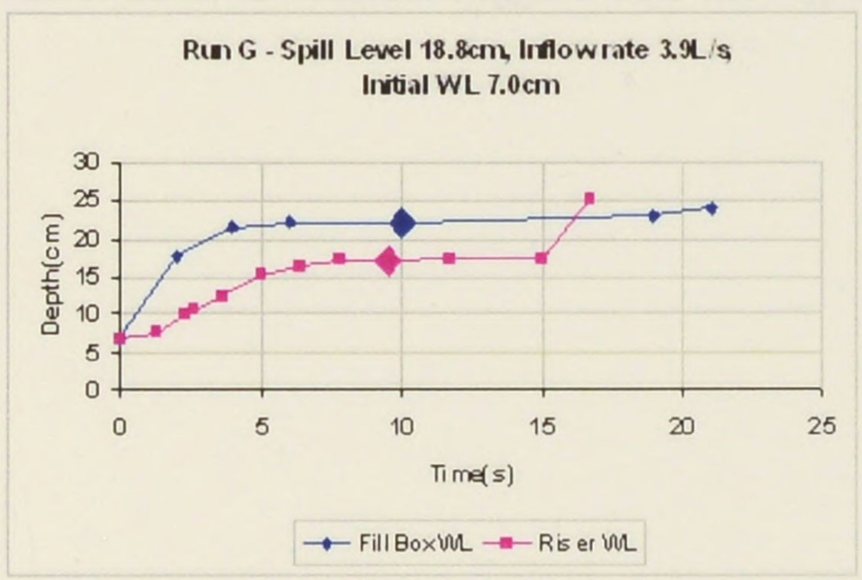

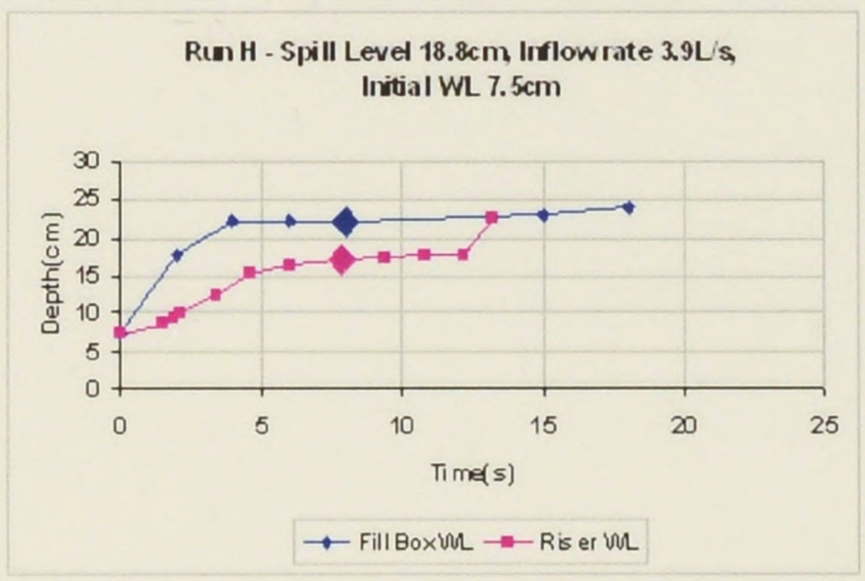

Figure 3.1: Plots of the Fill Box and Riser WL against time for 18.8 cm spill level. Large diamonds indicate IBD occurrence

The plots of the water levels at the fill box and riser shown in figure 3.1 are not conclusive in establishing a relationship between IBD occurrence and events on the system boundaries. The plots for settings A, B and E shows the fill box spilling and the surge tank WL stabilizing, without IBD occurrence. On the other hand, the remaining settings indicated the IBD occurrence by the time when the WL on the riser achieves a stable level. There's also a slightly tendency of IBD to occur sooner as the initial WL increases.

3.2 Results for the 23.8 cm spill level

The results for the experimental settings using the 23.8 cm spill level are presented in figure 3.2 and in table 3.3.

Table 3.3: Results of IBD occurrence for the 23.8 cm spill level

Setting	Inflow rate	Initial WL	IBD (Y/N)	Remarks/IBD location
A	3.9 L/s	6.2 cm	Yes	7.2 +/- 0.3 m from fill box
B	3.9 L/s	6.6 cm	Yes	8.7 +/- 0.3 m
C	3.9 L/s	7.0 cm	Yes	9.0 +/- 0.3 m
D	3.9 L/s	7.5 cm	Yes	9.3 +/- 0.3 m
E	3.1 L/s	6.2 cm	No	Undular front propagation
F	3.1 L/s	6.6 cm	Yes	8.7 +/- 0.3 m
G	3.1 L/s	7.0 cm	Yes	9.0 +/- 0.3 m
H	3.1 L/s	7.5 cm	Yes	9.3 +/- 0.3 m

Comparing these results with the ones obtained for the 18.8 cm spill level, one may notice that the IBD occurrence is more frequent. All the cases for the high inflow rates resulted in IBD, and only setting E for the low inflow rate resulted in no IBD occurrence. Table 3.3 confirms the tendency of the IBD to occur further downstream as the initial WL and the inflow rate increase.

The plots of the fill box and riser WL presented in figure 3.2 suggest that there's no connection between the event of the fill box spill and the IBD occurrence. As for the stabilization of WL at the riser, few settings show that the WL may increase even after IBD occurrence. As with the 18.8 cm spill level data, the results suggest that the higher the initial WL, the sooner the IBD will occur.

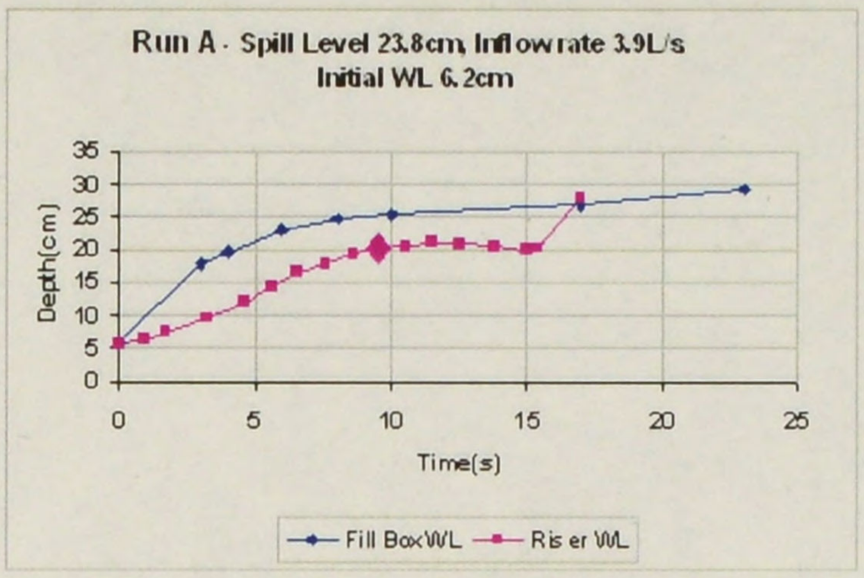

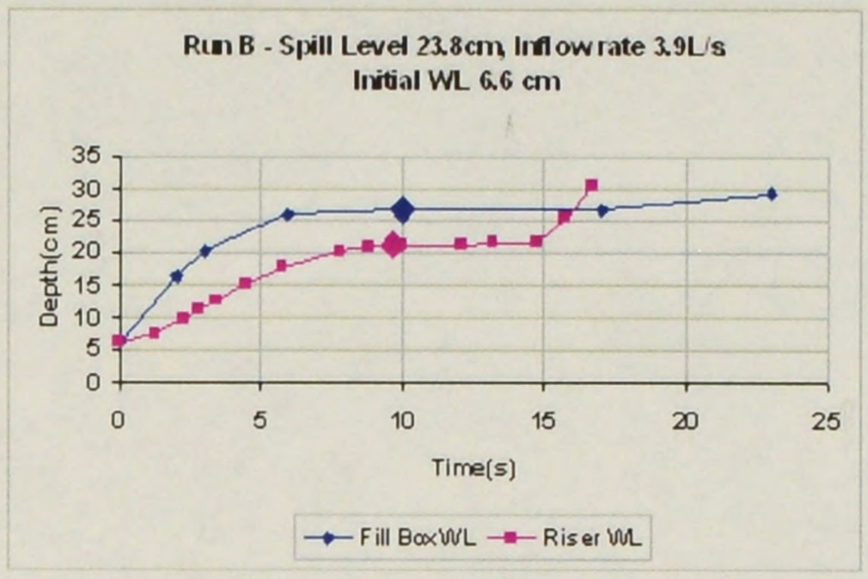

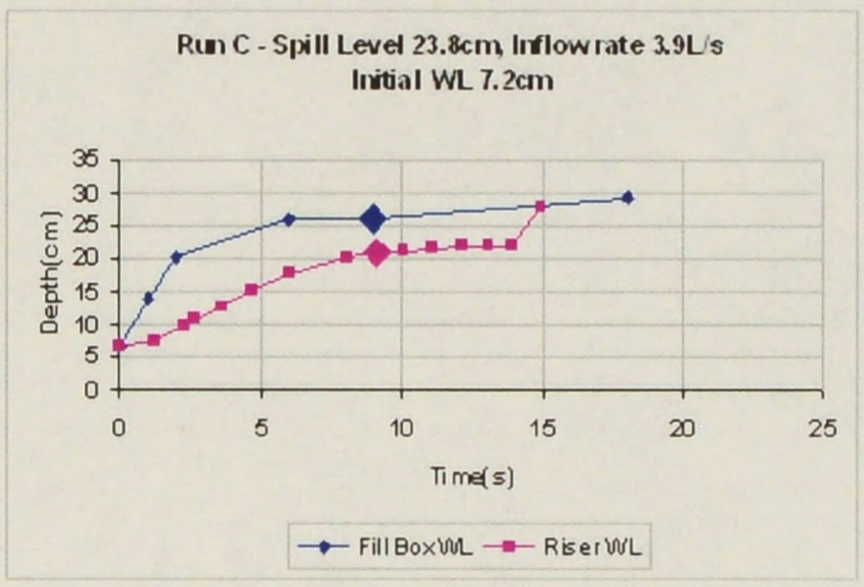

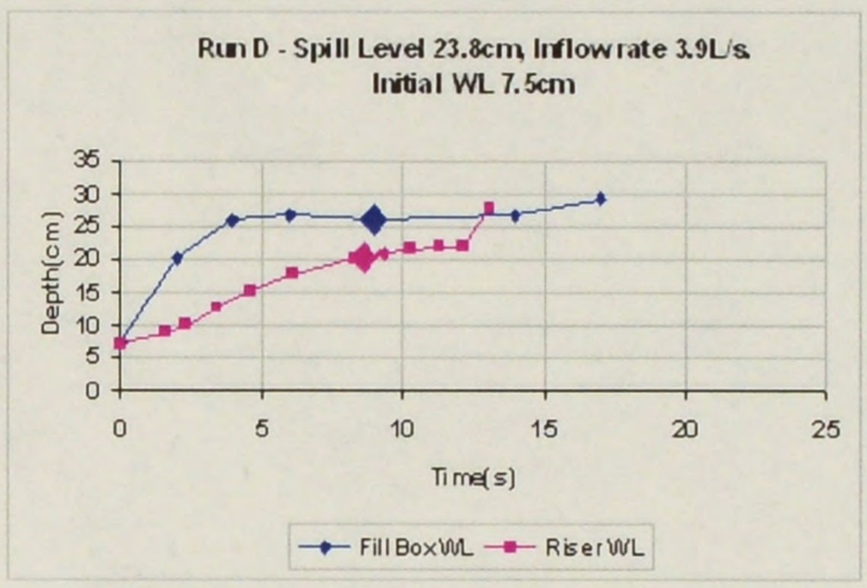

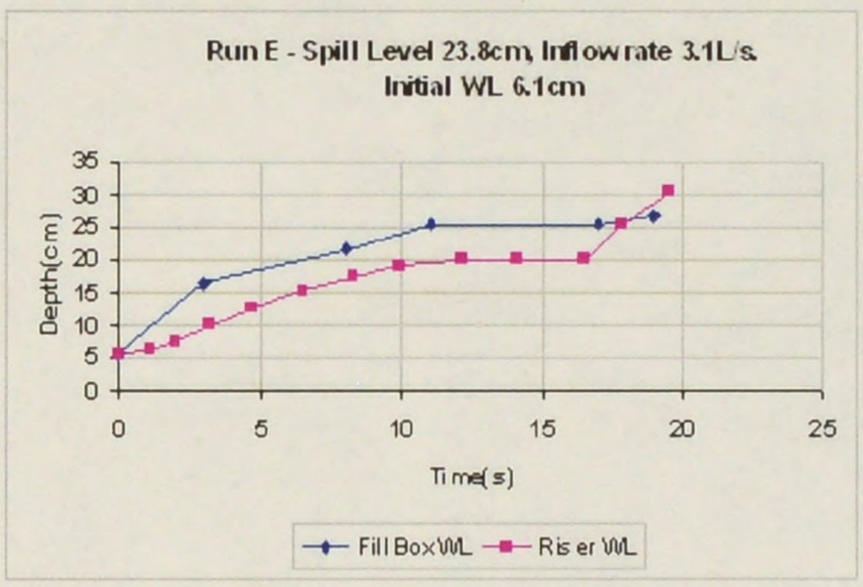

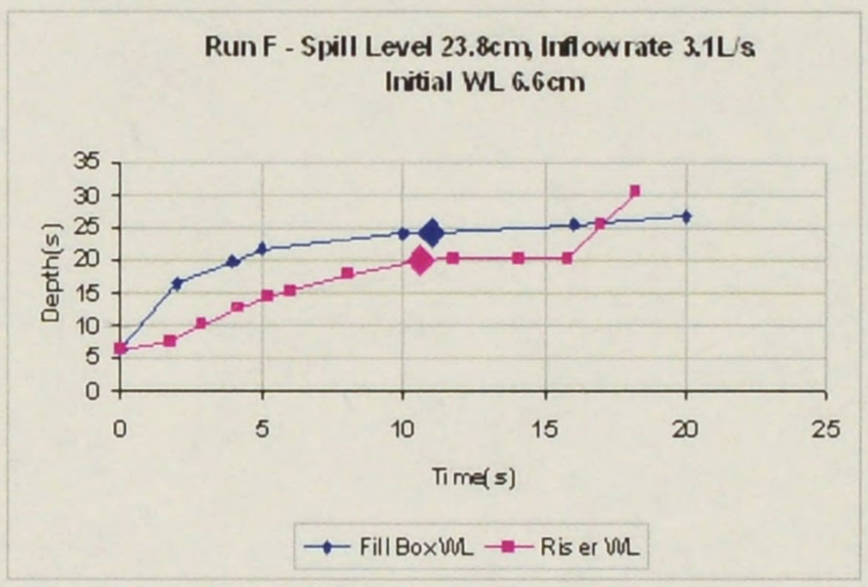

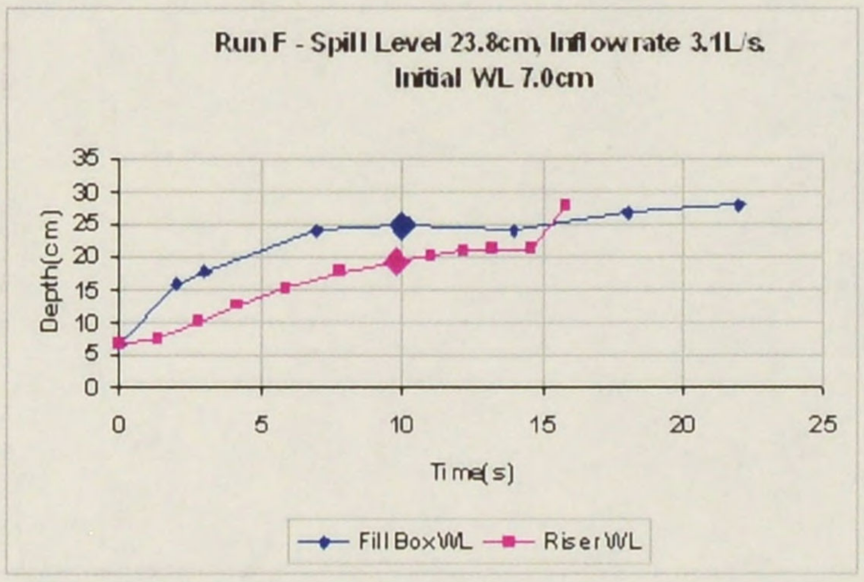

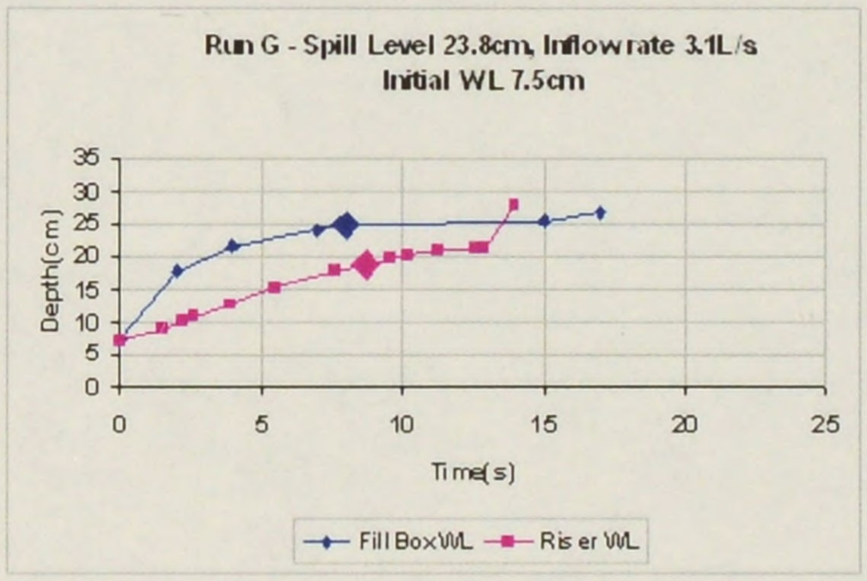

Figure 3.2: Plots of the Fill Box and Riser WL against time for 23.8 cm spill level. Large diamonds indicate IBD occurrence

3.3 Results for the 26.3 cm spill level

The results for the experimental settings using the 26.3 cm spill level are presented in figure 3.3 and in table 3.4.

Table 3.4: Results of IBD occurrence for the 26.3 cm spill level

Setting	Inflow rate	Initial WL	IBD (Y/N)	Remarks/IBD location
A	3.9 L/s	5.9 cm	Yes	Problem: air escaped at riser
B	3.9 L/s	6.5 cm	Yes	8.7 +/- 0.3 m
C	3.9 L/s	7.0 cm	Yes	9.3 +/- 0.3 m
D	3.9 L/s	7.5 cm	Yes	9.9 +/- 0.3 m
E	3.0 L/s	6.2 cm	No	Undular front propagation
F	3.0 L/s	6.6 cm	No	Transition to undular front
G	3.0 L/s	7.1 cm	Yes	9.0 +/- 0.3 m
H	3.0 L/s	7.6 cm	Yes	9.3 +/- 0.3 m

Results in table 3.4 shows that IBD occurred for all the high inflow conditions. There was a problem for setting A because during that setting the water depth approached the level of the gate located at the surge tank, allowing for air escape (bubbling) at that location. However, only half the settings with the lower inflow rate resulted in IBD. The result in setting F was interesting because the pipe-filling bore formed close to the surge tank, resulting in a very long air pocket trapped behind the bore. The results confirm that higher initial depths favors the occurrence of IBD.

The results for this spill level confirms that there is no relation between the spilling at the fill box and the IBD occurrence. This is because the IBD occurred even before the fill box started to spill. In association with the observations made for the lower spilling levels, one concludes that the fill box geometry does not explain the IBD occurrence. Again, in most settings IBD occurred, except for setting E when a undular front developed. The results also point to the occurrence of IBD even before the riser WL stabilizes. That would suggest that the riser geometry also wouldn't affect the IBD occurrence. The results with the highest spill level confirmed this.

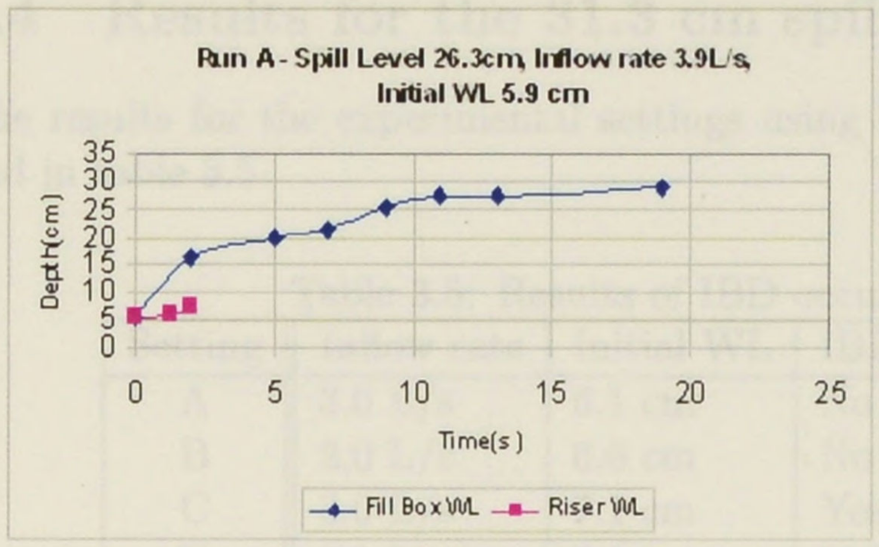

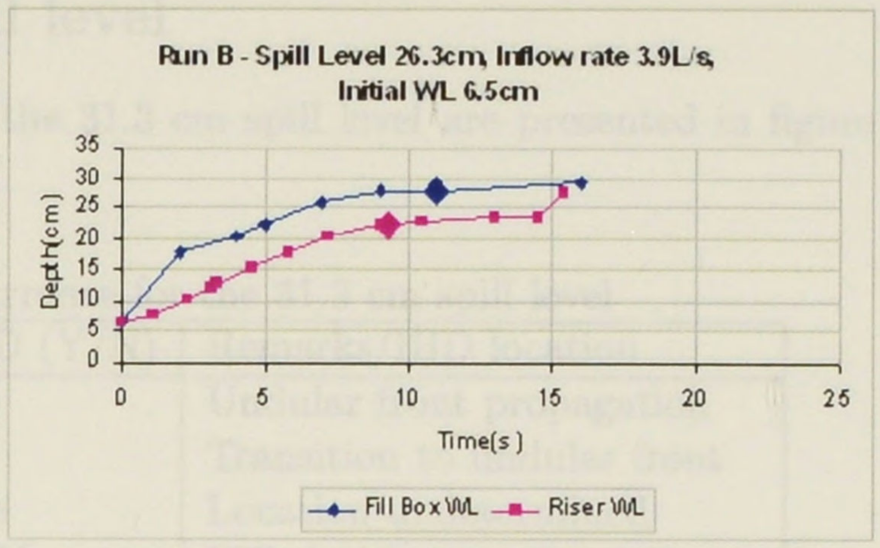

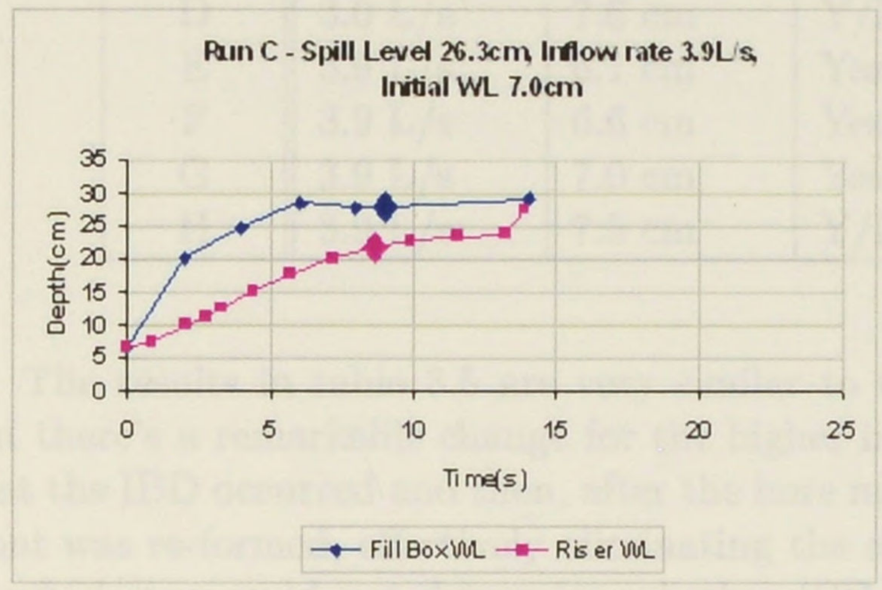

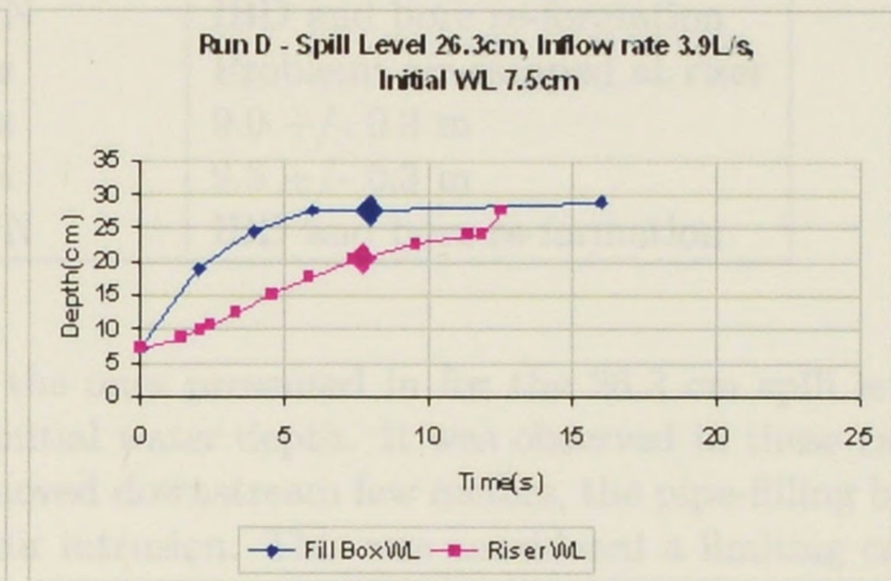

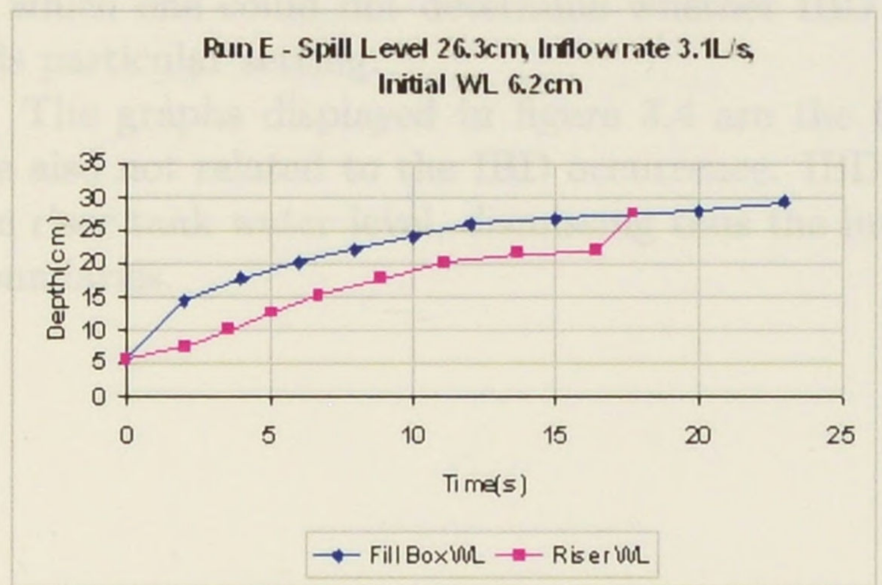

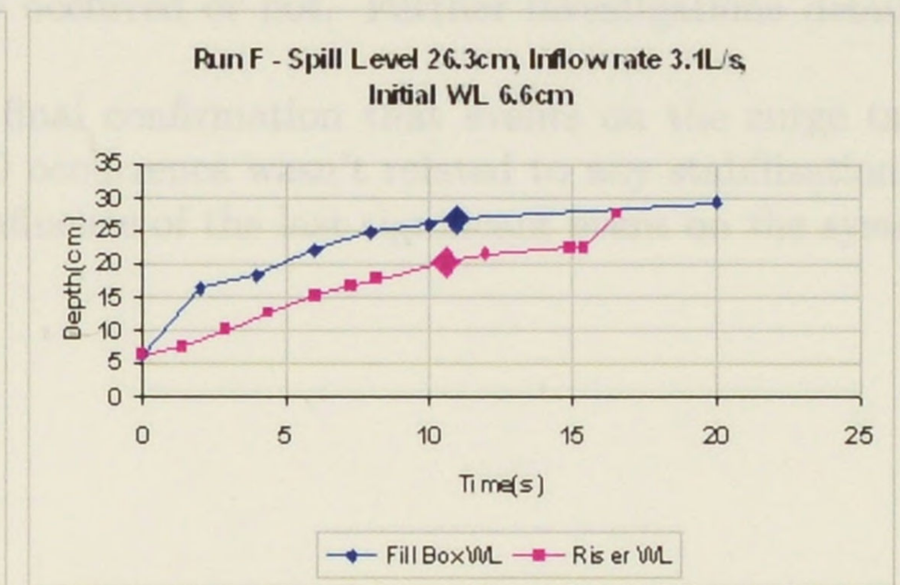

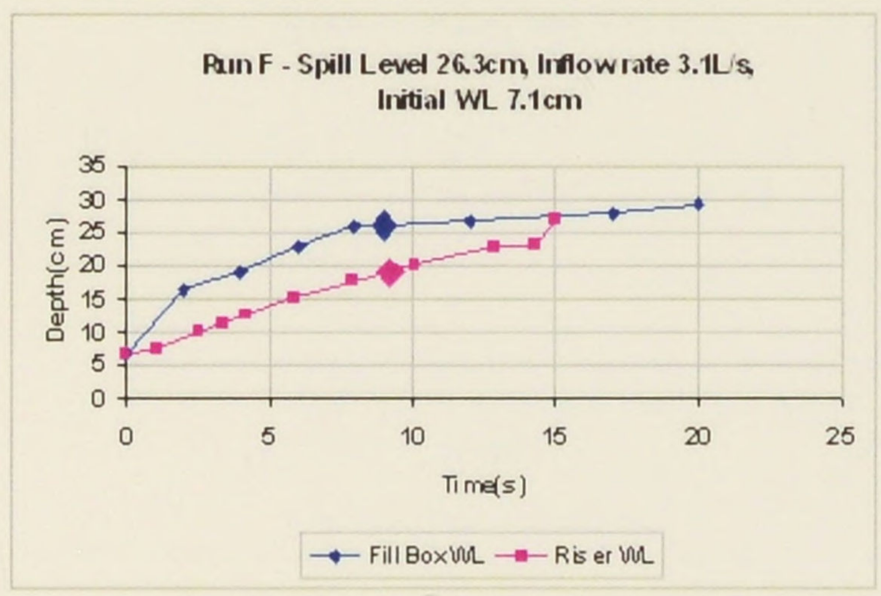

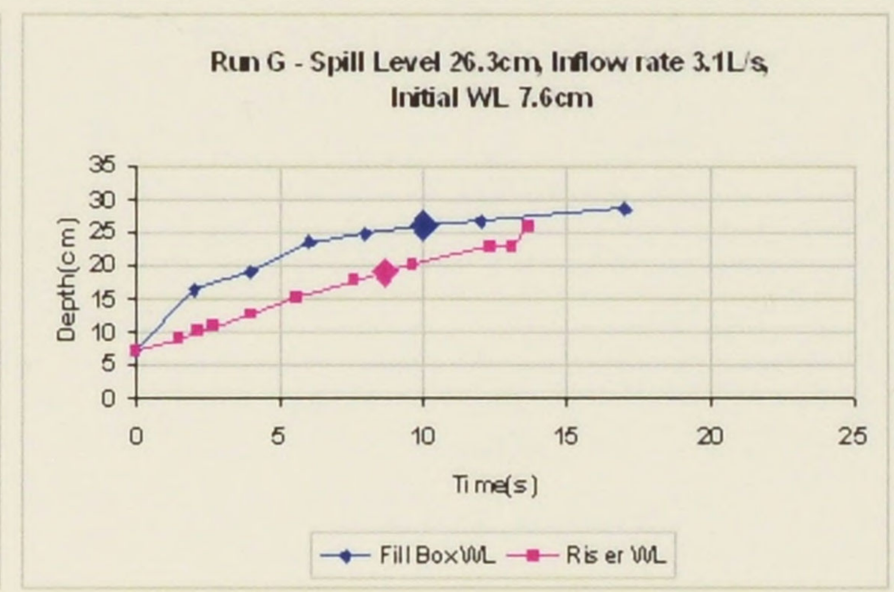

Figure 3.3: Plots of the Fill Box and Riser WL against time for 26.3 cm spill level. Large diamonds indicate IBD occurrence

3.4 Results for the 31.3 cm spill level

The results for the experimental settings using the 31.3 cm spill level are presented in figure 3.4 and in table 3.5.

Table 3.5: Results of IBD occurrence for the 31.3 cm spill level

Setting	Inflow rate	Initial WL	IBD (Y/N)	Remarks/IBD location
A	3.0 L/s	6.1 cm	No	Undular front propagation
B	3.0 L/s	6.6 cm	No	Transition to undular front
C	3.0 L/s	7.1 cm	Yes	Location undetermined
D	3.0 L/s	7.6 cm	Y/N	IBD and bore re-formation
E	3.9 L/s	6.1 cm	Yes	Problem: air escaped at riser
F	3.9 L/s	6.6 cm	Yes	9.0 +/- 0.3 m
G	3.9 L/s	7.0 cm	Yes	9.3 +/- 0.3 m
H	3.9 L/s	7.5 cm	Y/N	IBD and bore re-formation

The results in table 3.5 are very similar to the ones presented in for the 26.3 cm spill level, but there's a remarkable change for the higher initial water depth. It was observed in these cases that the IBD occurred and then, after the bore moved downstream few meters, the pipe-filling bore front was re-formed, effectively eliminating the air intrusion. This was considered a limiting case, in which one could not determine whether IBD occurred or not. Further investigations detailed this particular setting.

The graphs displayed in figure 3.4 are the final confirmation that events on the surge tank are also not related to the IBD occurrence. IBD occurrence wasn't related to any stabilization of the riser tank water level, dismissing thus the influence of the last significant event on the system boundaries.

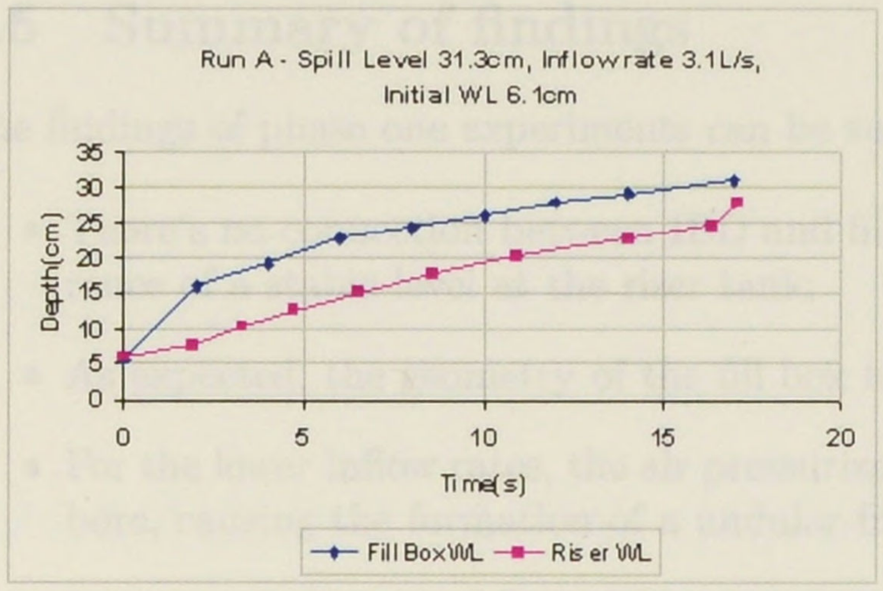

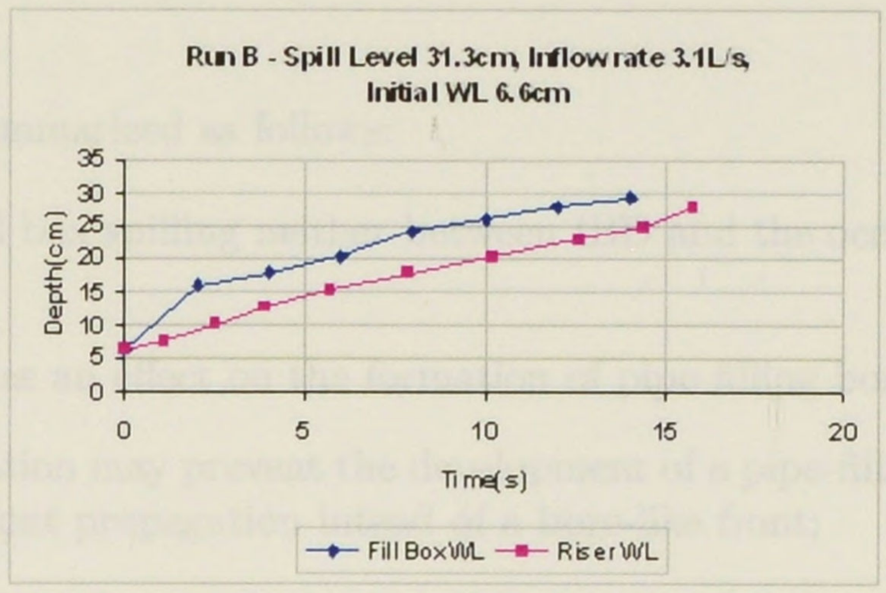

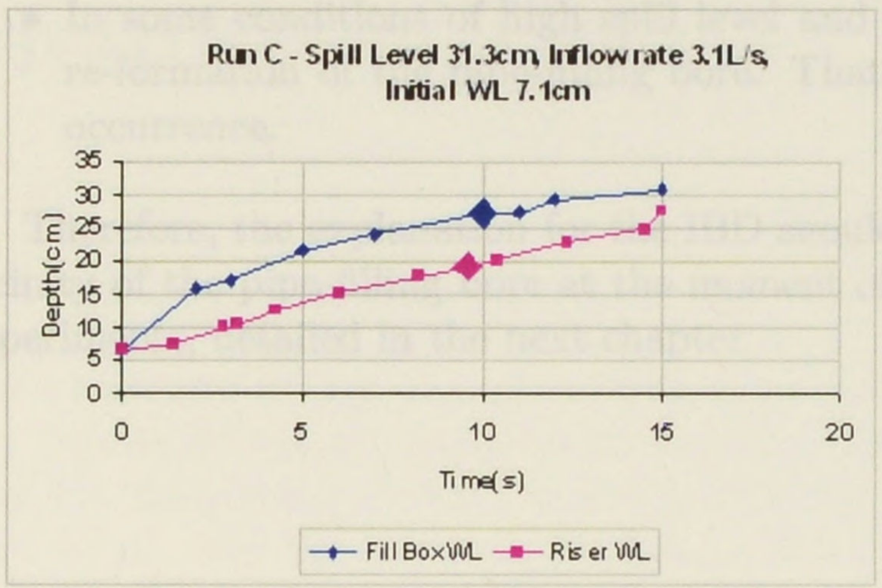

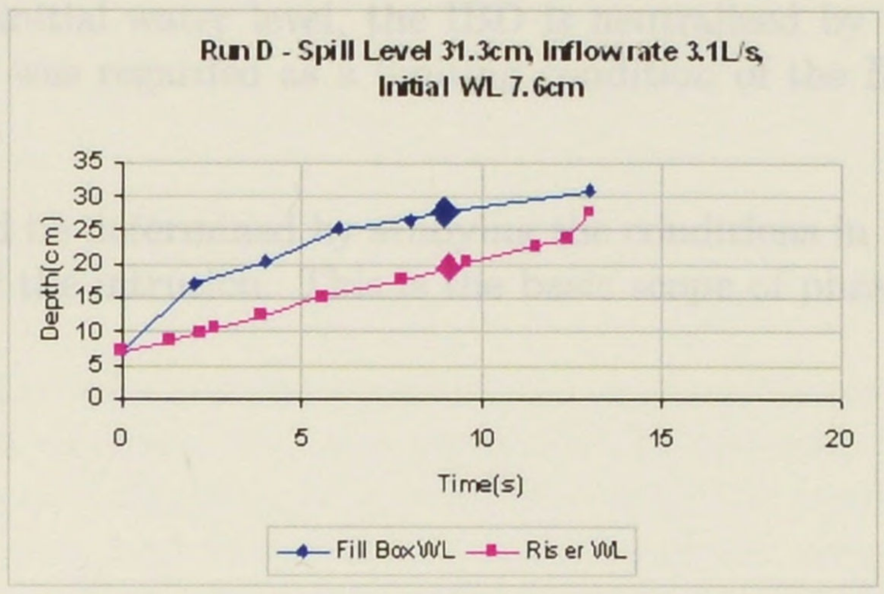

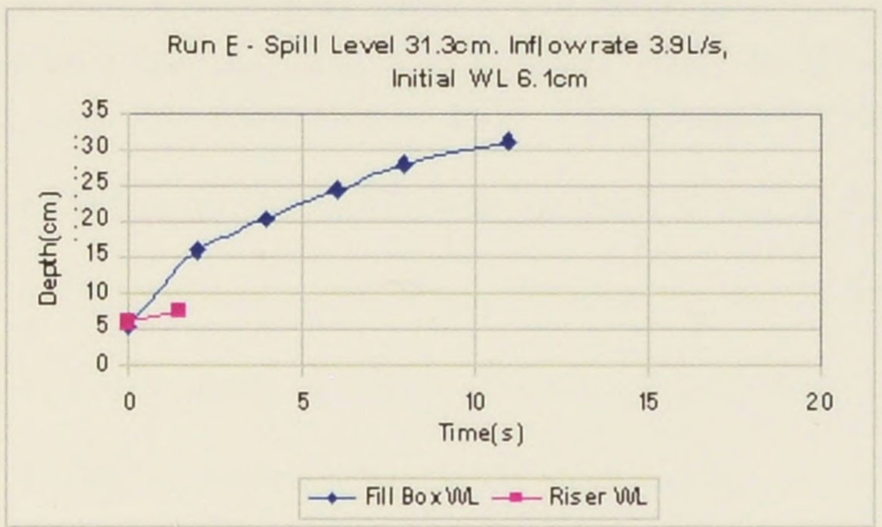

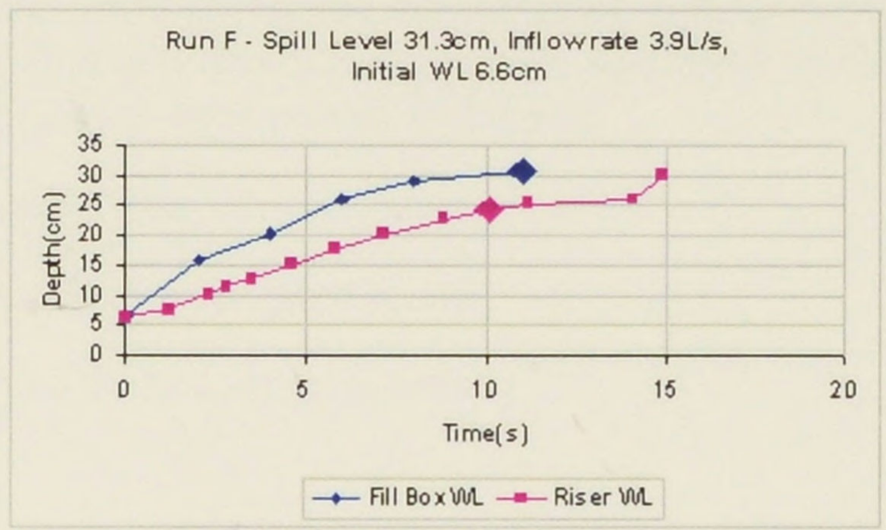

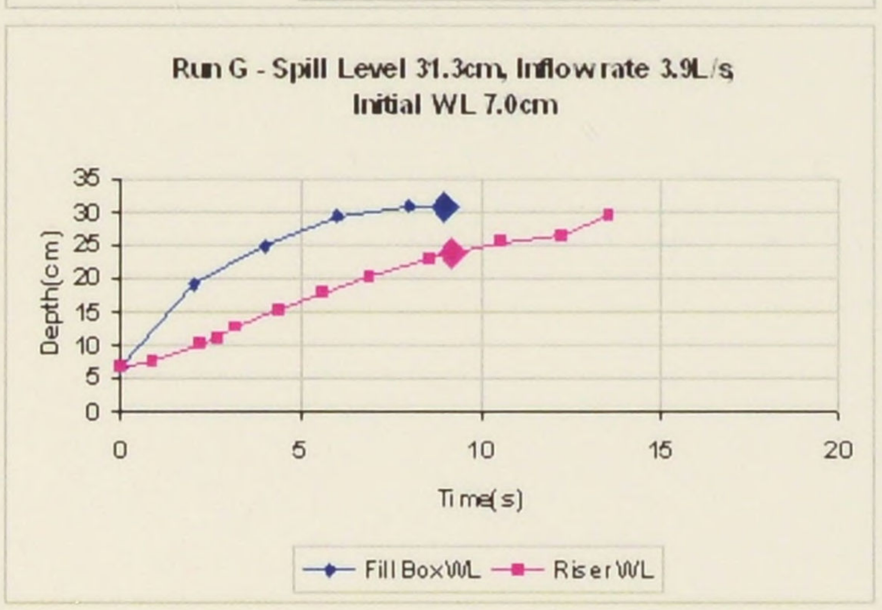

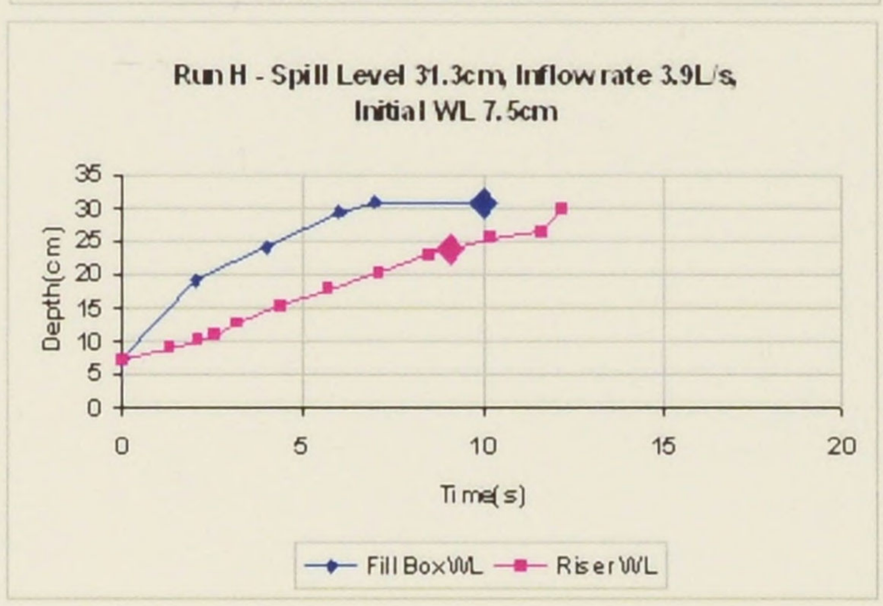

Figure 3.4: Plots of the Fill Box and Riser WL against time for 31.3 cm spill level. Large diamonds indicate IBD occurrence

3.5 Summary of findings

The findings of phase one experiments can be summarized as follows:

- There's no connection between IBD and fill box spilling neither between IBD and the occurrence of a stable level at the riser tank;
- As expected, the geometry of the fill box has an effect on the formation of pipe-filling bore;
- For the lower inflow rates, the air pressurization may prevent the development of a pipe-filling bore, causing the formation of a undular front propagation intead of a bore-like front;
- In some conditions of high spill level and initial water level, the IBD is neutralized by the re-formation of the pipe-filling bore. That was regarded as a limiting condition of the IBD occurrence.

Therefore, the explanation for the IBD should be determined by studying the conditions in the vicinity of the pipe-filling bore at the moment of the intrusion. This is the basic scope of phase 2 experiments, detailed in the next chapter.

Chapter 4

Detailing flow conditions in the vicinity of IBD

4.1 Pressure measurements across IBD

The phase two of the "interface breakdown" experiments aimed to detail the flow conditions at the vicinity of the air intrusion in several conditions were IBD was observed. To promote this analysis, the pressures ahead of and behind the pipe-filling bore were measured with the pressure transducers, and the water depth changes in the riser tank were recorded with the digital camera.

It was decided to narrow the original 32 settings from phase one experiments to exclude cases in which undular fronts occurred. The resulting 16 experimental settings are displayed in Table 4.1, each one resulting in IBD. The measurement devices were placed as follows:

- Transducer e11372 was located at 8.5 m from fill box, at pipe crown;
- Transducer e11402 was located at 9.8 m from fill box, at pipe crown;
- Transducer e11348 was located at 14.1 m from fill box, at pipe crown;
- Digital camcorder at the riser tank;

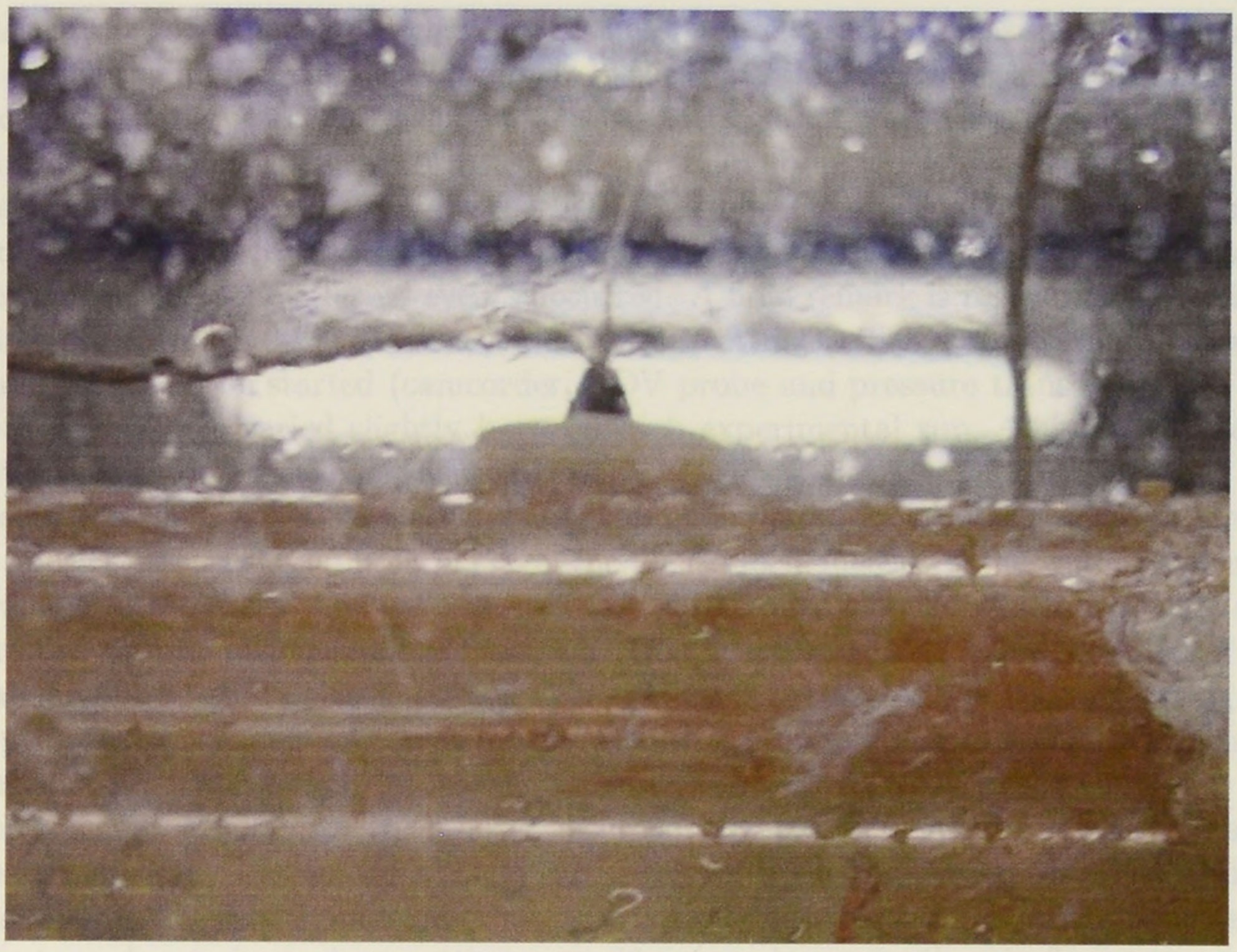

Figure 4.1: Photograph of transducer e11348 mounted at 14.1 m from fill box, at pipe crown

Table 4.1: Experimental settings considered for IBD experiments - phase two

Setting	Spill level	Inflow Rate	Initial WL
A	18.8 cm	3.1 L/s	6.7 cm
B	18.8 cm	3.1 L/s	7.3 cm
C	18.8 cm	3.9 L/s	6.7 cm
D	18.8 cm	3.9 L/s	7.3 cm
E	23.8 cm	3.1 L/s	6.7 cm
F	23.8 cm	3.1 L/s	7.3 cm
G	23.8 cm	3.9 L/s	6.4 cm
H	23.8 cm	3.9 L/s	7.4 cm
I	26.3 cm	3.1 L/s	6.6 cm
J	26.3 cm	3.1 L/s	7.3 cm
K	26.3 cm	3.9 L/s	6.4 cm
L	26.3 cm	3.9 L/s	7.2 cm
M	31.3 cm	3.1 L/s	6.5 cm
N	31.3 cm	3.1 L/s	7.2 cm
O	31.3 cm	3.9 L/s	6.4 cm
P	31.3 cm	3.9 L/s	7.2 cm

For each of the conditions studied, a plot of the pressure variation measured by the transducers over time during the filling event was obtained. In the same plot, the water level variation measured with the camera at the riser was graphed. On the latter graph there are two markers. The first mark signals the moment when the formation of pipe-filling bore (PFB) was first noticed, while the second marker signals the moment when the IBD occurred. Those visual observations were subject to some imprecision since it was relatively hard to move as fast as the bore and at the same time determine exactly when the referred events occurred. A final remark is regarding the variable time offset in the pressure build-up between experimental settings. There was various measurements devices that needed to be started (camcorder, ADV probe and pressure transducers) in each run, and the start-ups times varied slightly between each experimental run. This in turn resulted in time offsets between different experimental runs.

Because the transducers were placed on the top of the pipe, they initially gaged the variations in the air phase pressure. Upon bore passage, the transducers measured the water pressure at that location, unless in the cases they were located in the IBD intrusion, in which case they continued to measure the air pressure inside the intrusion. One characteristic of the experimental results is that the air pressure variation is smoother than the water pressure. It is also interesting to notice the early pressure oscillations on the air phase, resulting probably due to transients during the air flow initiation.

One unexpected result also was relative discrepancies between pressure transducers readings that appeared in some cases within a single run. Because of the high speed of the acoustic wave in the air, one wouldn't expect siginificant differences in the results from the air pressure measurements among the transducers in a given setting even if energy losses in the air flow were considered. Nevertheless, in some cases such discrepancies between transducers readings were detected. It was later determined that this problem was connected with the fact that the transducers experience phase change during the measuring process. It is likely that small water droplets present on the diaphragm of these high sensitivity transducers before the flow initiation affected the accuracy of the readings. Similarly, after the bore passage, it is possible that small air bubbles located on the transducer's face affected the accuracy of the pressure readings. This problem was finally identified at the end of the phase two experiments, and corrections were implemented to avoid this issue prior to phase three of IBD experiments.

4.2 IBD phase two experiments - Results

The pressure measurements from experimental settings A, B, C and D from table 4.1 are shown in figure 4.2.

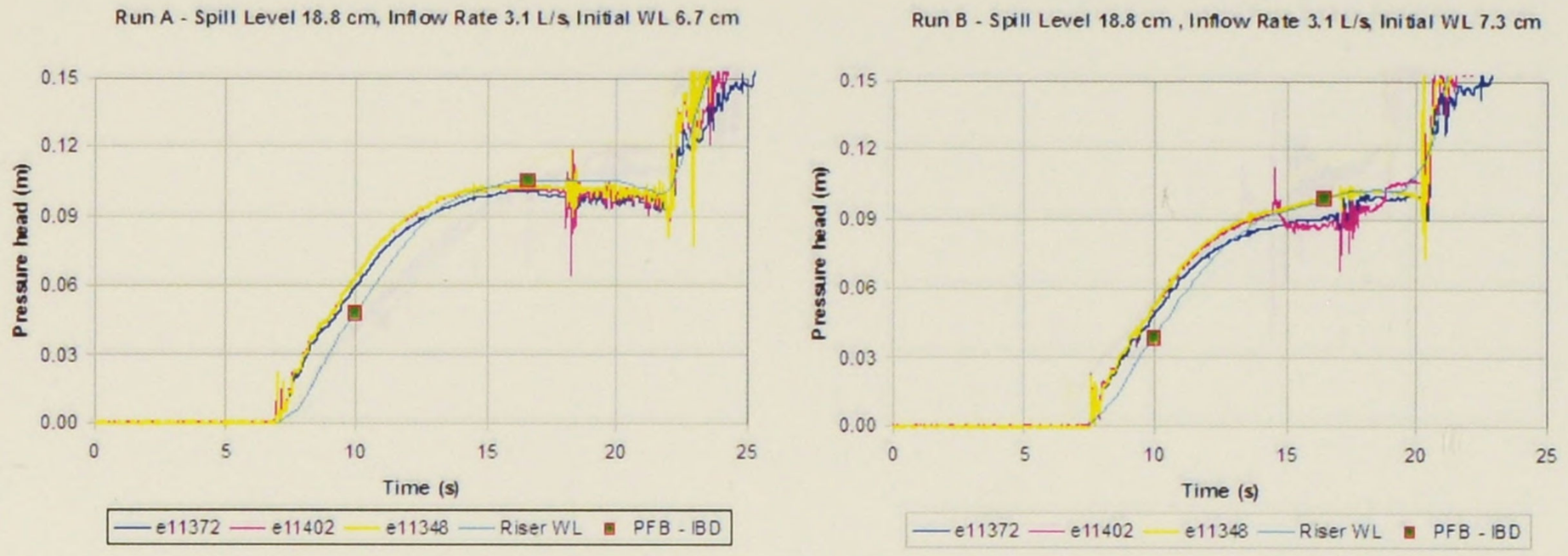

Figure 4.2: Pressure head for phase two experiments - settings A, B, C and D

The results indicate that the pipe filling bore formation in each setting is not so "immediate" as initially thought, and in some cases may take up to 4 seconds to occur. As mentioned, there's some discrepancies in the pressure results between the different settings, particularly in setting C. Settings A and C are examples of the low initial water level conditions. The results of these two settings are similar in the sense they indicate initial increase of the air pressure followed by few high frequency pressure oscillations, associated with air bubble expulsion. Additionally, in these settings all the transducers were located downstream from the IBD occcurrence. There was no significant differences in the results obtained with the transducers, and as a result no insight with respect to the IBD occurrence was gained.

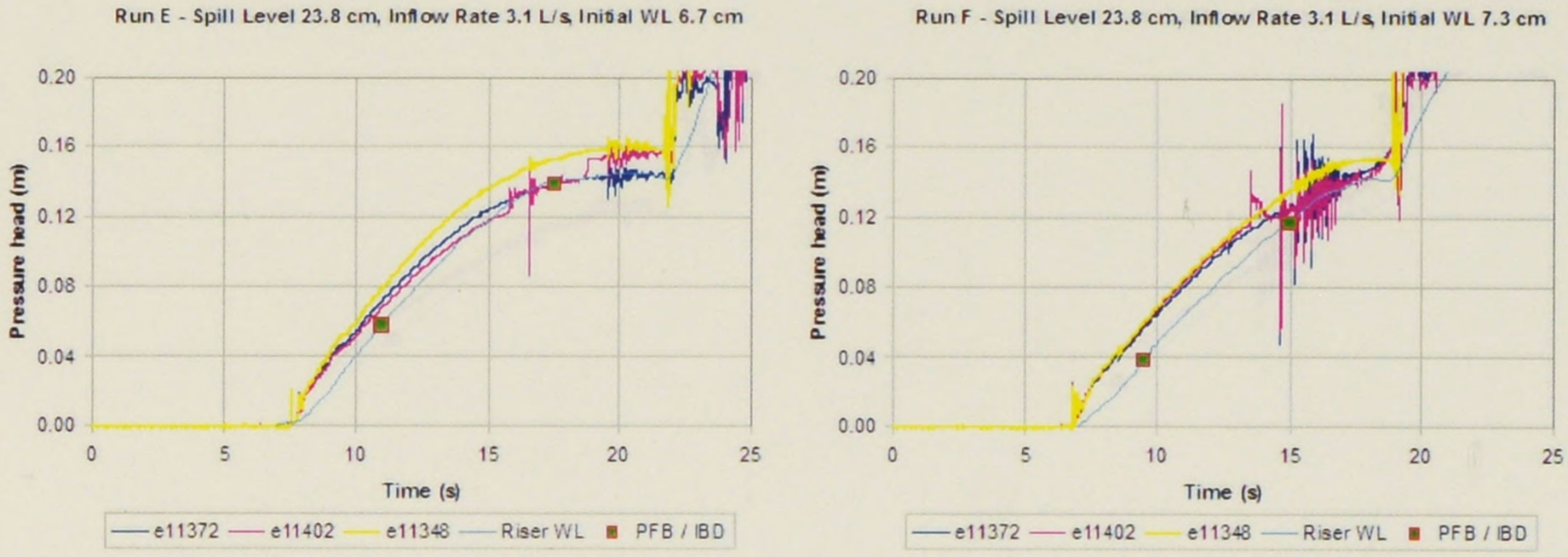

Figure 4.3: Pressure head for phase two experiments - settings E, F, G and H

Settings B and D, with higher initial WL, offered more intesting information on what happens during IBD events. That is because some transducers (e11402 or e11372) were location upstream from the IBD location. The pressure measurements at those points indicate a sudden drop in the pressure around the time when the IBD occurred. This decrease in the pressure proved to be a "signature" of the IBD occurrence for data obtained with the transducers. Those results explained the cause for IBD occurrence, as will be elaborated below.

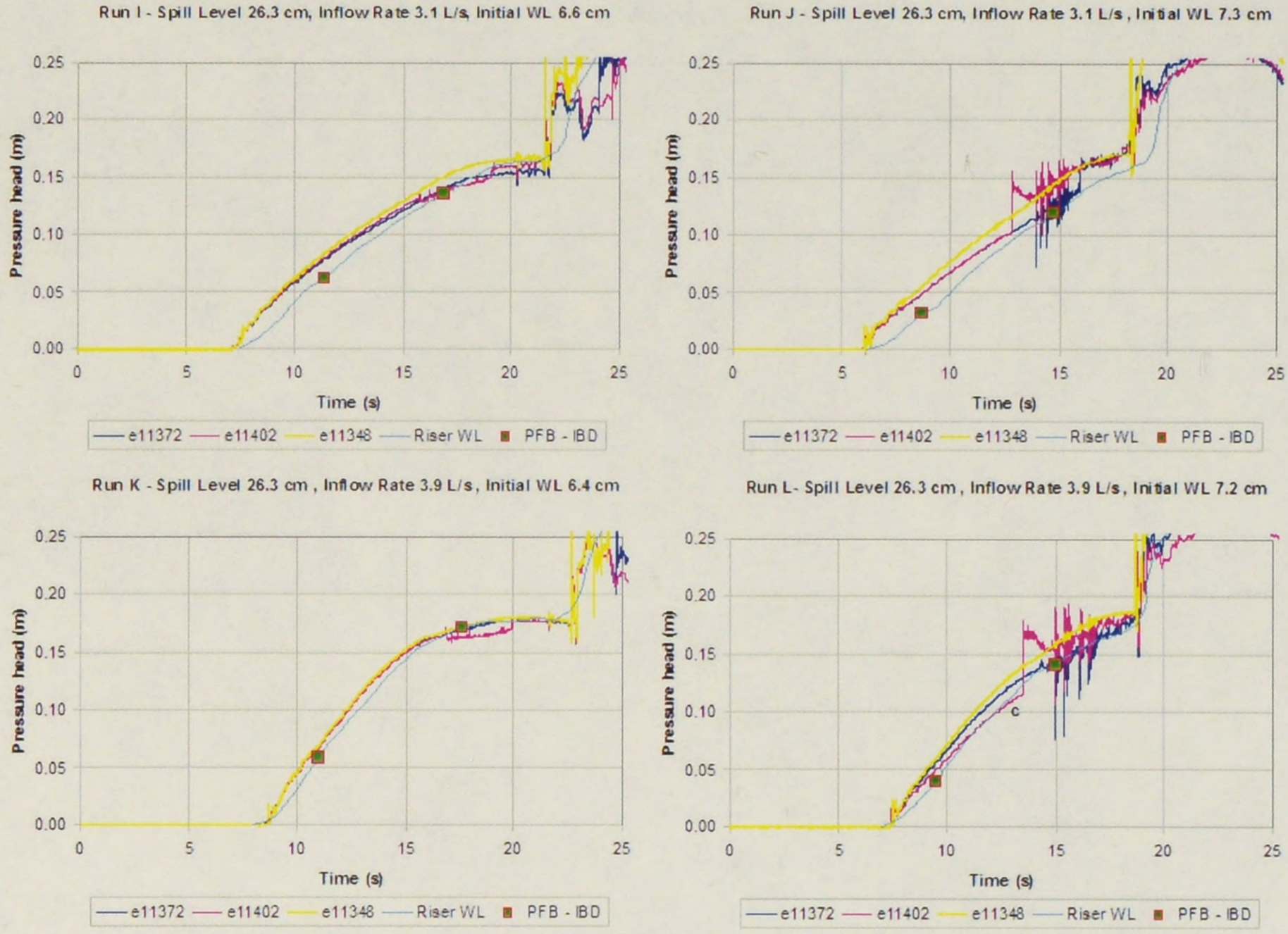

Figure 4.4: Pressure head for phase two experiments - settings I, J, K and L

The results for most of the remaining experimental settings for the higher spill levels indicated the occurrence of IBD with the correspondent pressure "signature". In few cases there were some discrepancy issues, but that did not prevent the detection of the sudden drop in the pressure data from the transducers around the time when IBD occurred. For some of the settings with higher initial water level, it is easy to notice events such as the passage of the pressurization bore and pressure oscillations due to bubbling in the fill box. The transducer located at the end of the pipe (e11348) yielded data with comparatively smaller pressure oscillations, and that is because this transducer was measuring air pressure during the whole pipe filling event.

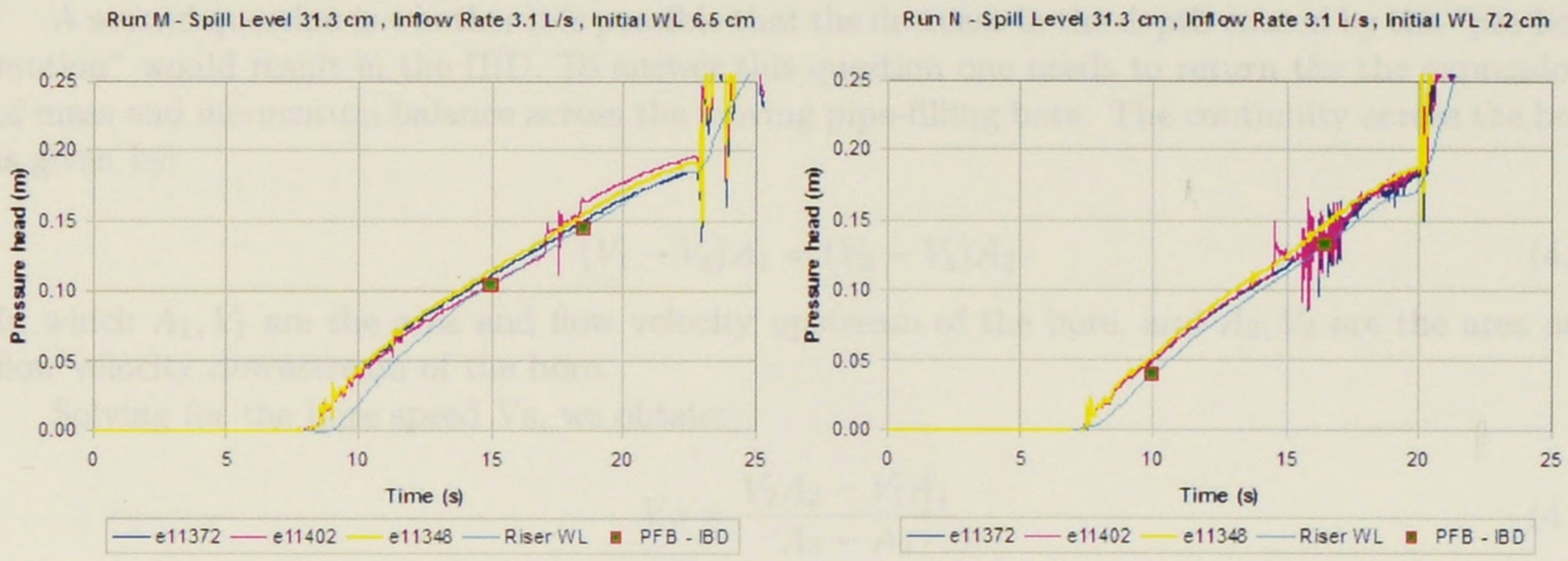

Figure 4.5: Pressure head for phase two experiments - settings M, N, O and P

4.3 Analysis of the Results

The experiments promoted in phase two of the experiments shed light on what occurs at the pressurization bore during a IBD event. The characteristics of the bore are altered, since a localized drop in the measured pressure at the time when the IBD occurred was detected . This pressure drop was regarded as the "signature" of IBD occurrence in the data provided by the transducers.

This poses some questions. One question is what could cause the observed pressure drop at the pressurization bore. One may speculate that the "pre-bore motion" (figure 1.2) could be a possible cause for the pressure drop, since it results in a upstream propagating cavity on the free surface portion of the flow.

The possibility of other flow features to alter the behavior of the pressurization front was observed in previous investigations. Cardle and Song (1988) relate the occurrence of "interface reversal", when the direction of the pressurization bore was reversed by the flow conditions at the bore vicinity. Unlike the IBD, the cause of the "interface reversal" is not related to the air pressurization. It seems that this reversal is generated by a pressure decrease on the pressurized side of the pipe-filling bore.

A second question is whether it is possible that the decrease in the depth caused by the "pre-bore motion" would result in the IBD. To answer this question one needs to return the the expressions of mass and momentum balance across the moving pipe-filling bore. The continuity across the bore is given by:

$$(V_1 - V_s)A_1 = (V_2 - V_s)A_2 \tag{4.1}$$

In which A_1, V_1 are the area and flow velocity upstream of the bore, and A_2, V_2 are the area and flow velocity downstream of the bore.

Solving for the bore speed Vs, we obtain:

$$Vs = \frac{V_2A_2 - V_1A_1}{A_2 - A_2} \tag{4.2}$$

The momentum conservation across the bore can be written as:

$$g\left[A_2\bar{y}_2 - A_1\left(\frac{D}{2} + Z - H_{air}\right)\right] = A_1(V_1 - V_s)(V_2 - V_1) \tag{4.3}$$

In which $\bar{y}_2$ is the depth of the centroid in the free surface region, Z is the pressure head above the pipe crown on the water-filled side of the bore, and H_{air} is the air phase pressure head.

After introducing equation 4.2 into equation 4.3 and algebraic manipulations, we arrive at the following expression that relates Z to the other variables:

$$Z = \frac{\bar{y}_2A_2}{A_1} - A_2\frac{(V_1 - V_2)^2}{A_2 - A_1} - \frac{D}{2} + H_{air} \tag{4.4}$$

In order for IBD occur, the value of Z from Equation 4.4 should drop below the value of H_{air}, in which case intrusion of air will occur along the top of the pipe. To determine whether this is possible, one would need the velocity data across the pipe-filling bore, and that type of measurement wasn't promoted in these experiments. That was promoted in phase three experiments using the ADV probe.

We can, however, develop a rough estimatation of whether IBD would occur using the data from the settings we measured in the 9.4 cm pipeline. Using, for instance, the data from setting D, assume the depth downstream from the IBD location equal to 6.5 cm, decreased from the original 7.3 cm due to the "pre-bore motion". With this depth assumed, the resulting centroid depth $\bar{y}_2$ is 3.7 cm and the area downstream the bore A_2 is $5.1410^{-3}m^2$, while upstream the bore we have the centroid $\bar{y}_1$ = D/2 = 4.8 cm and area $A_1 = 6.9410^{-3}m^2$. Replace these estimated values in equation 4.4, the resulting equation is (in SI units):

$$Z - H_{air} = 0.2629V_1^2 - .5257V_1V_2 + .2629V_2^2 - .017740; \tag{4.5}$$

Assuming only positive velocities, the right hand side of the equation 4.5 is zero if $V_1 - V_2 =$ 0.2747 m/s. This represents the minimum velocity difference across the bore required to prevent the air intrusion. Because the "pre-bore motion" causes a sudden increase of V_2, this may result in the air intrusion. Indeed, after plotting $Z - H_{air}$ surface against the V_1, V_2 velocities (figure 4.6), the value of $Z - H_{air}$ may even drop below zero depending on the values of the velocities. This suggests that the cause for the IBD may be indeed the interaction between the "pre-bore motion"

and the pipe-filling bore. The confirmation of this hypothesis is the motivation for the phase three of experiments regarding the IBD phenomena.

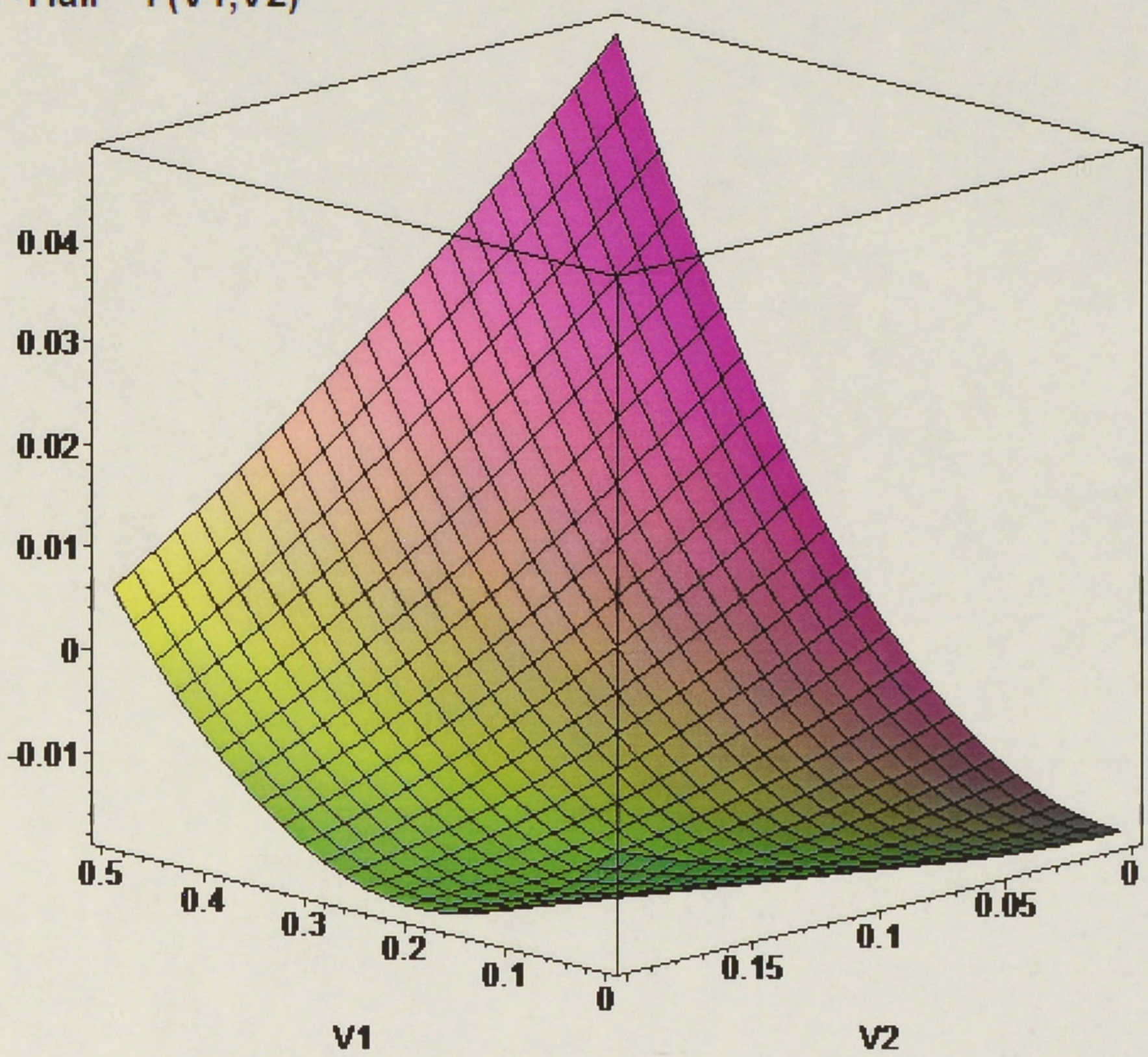

Figure 4.6: Plot of $Z - H_{air}$ as a function of V_1 and V_2, assuming the conditions on setting D with depth downstream of the bore of 6.5 cm.

Chapter 5

Predicting IBD occurrence

The findings of phase two experiments suggested that the IBD occurrence is caused by the interaction between the pipe-filling bore and the "pre-bore motion" feature, and to confirm this phase three experiments were promoted.

In these experiments, the experimental settings were further narrowed to include only four different settings, namely runs based on conditions C, D, G and H from table 3.5. The reason for this choice is that while runs C and G are clear examples of IBD occurrence, runs D and H represent limiting cases, in which IBD occurs but later on the pressurization bore reforms. For each of these runs, three repetitions were promoted to assure repeatability.

The experimental apparatus was changed. Two pressure transducers were relocated to the bottom of the pipe to minimize the problem with the results resulting from phase change, as discussed in the previous chapter. It was decided to place a pair of transducers (top and bottom) at the pipe end (figure 5.1). The remaining transducer was placed at the bottom at the 9.6 m station. The only transducer kept in the pipe top aimed (e11348) aimed to gage the air phase pressure at the pipe end during the filling process.

One additional change in the experimental setting was the placement of the ADV probe also at the 9.6 m station to measure the water velocity during the rapid filling process. Figure 5.2 shows how the ADV probe and the transducers were mounted at that location. Finally, the digital camera was placed at the 14.1 m station to measure the depth changes at that location.

These experiments were promoted in parallel with the development of a numerical model to solve the Saint-Venant equations including the effects of the air phase pressurization. This chapter presents a brief description of the numerical model used in the predictions of the IBD occurrence, and these predictions are included for each one of the experimental settings considered

5.1 Phase three experiments: Results

The four different experimental settings considered in the phase three experiments are presented in table 5.1. Each of the four settings were repeated three times to assure repeatability and consistency of the results.

Figure 5.1: Pair of transducers (top and bottom) placed at the 14.1 m station

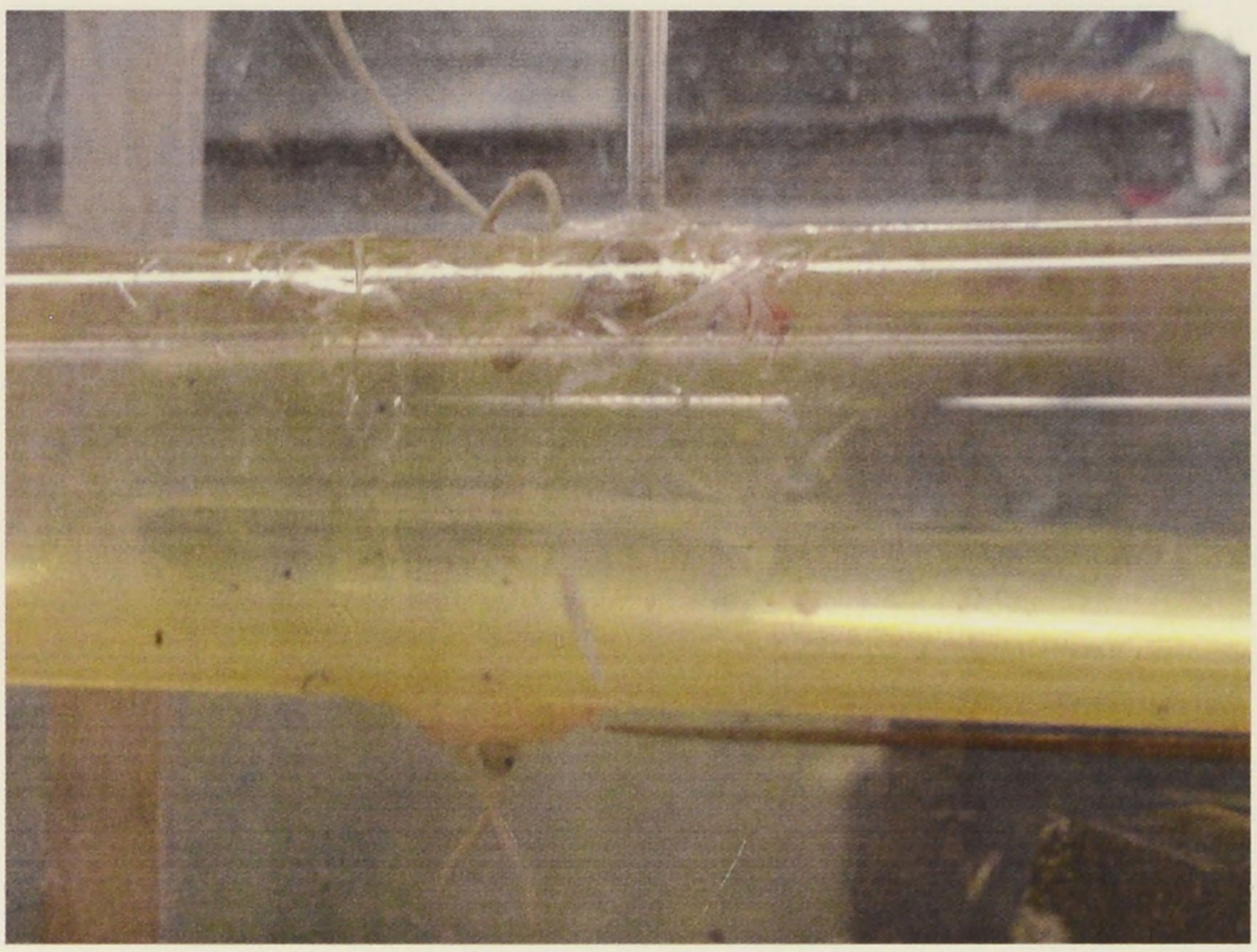

Figure 5.2: Transducer and ADV probe located at the 9.6 m station

Table 5.1: System variables considered for IBD experiments - Phase three

Setting	Spill level	Inflow Rate	Initial WL	IBD occurence
A	31.3 cm	3.1 L/s	7.1 cm	Yes
B	31.3 cm	3.1 L/s	7.6 cm	Yes, but bore reforms
C	31.3 cm	3.9 L/s	7.1 cm	Yes
D	31.3 cm	3.9 L/s	7.6 cm	Yes, but bore reforms

The results for the velocity measurements using the ADV probe for each of the settings are shown in figure 5.3. In general the results show initially no velocity at the 9.6 m station. After flow initiation, an increase in the velocity is noticed, resulting from the "pre-bore motion" feature. Following, there's a sudden increase in the velocity, resulting from the pressurization bore arrival. Finally, the oscillations in the velocity reflects the water motion observed on the surge tank.

There's an interesting observation in velocity measurements for the lower initial water level. There are few deviations of the general velocity oscillations pattern after the bore arrival at the surge tank. It was found after visual observations that these deviations are associated with the passage of air pockets at the location of the ADV probe. These deviations are not exactly the same between the repetitions of each experimental setting. This is in agreement with the expectation that the movement of air pockets has a localized effect on the water flow velocities. The lack of deviations for results with higher initial water level is due to the smaller air pockets observed in these settings.

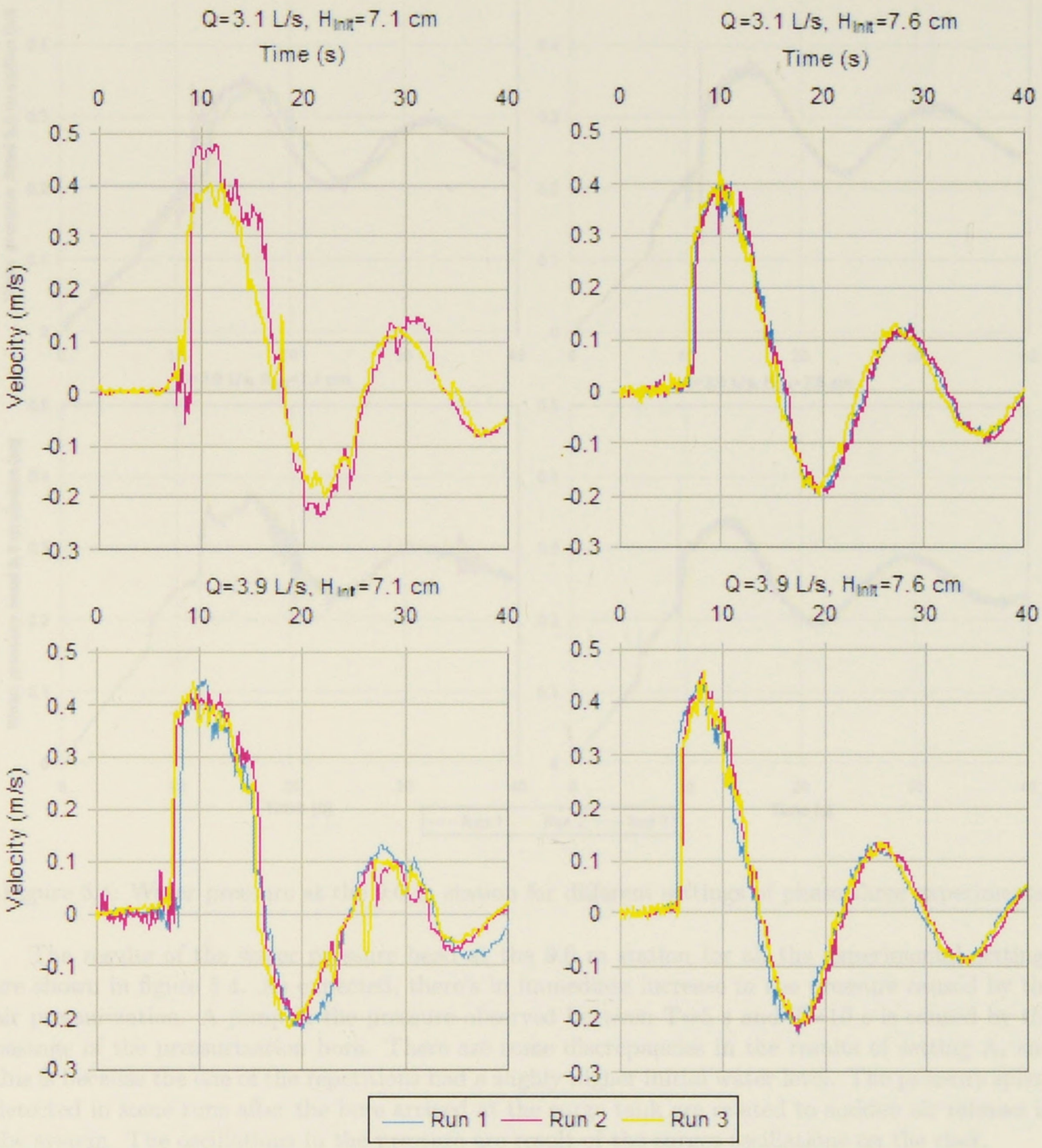

Figure 5.3: Velocity measurements at the 9.6 m station for different settings of phase three experiments

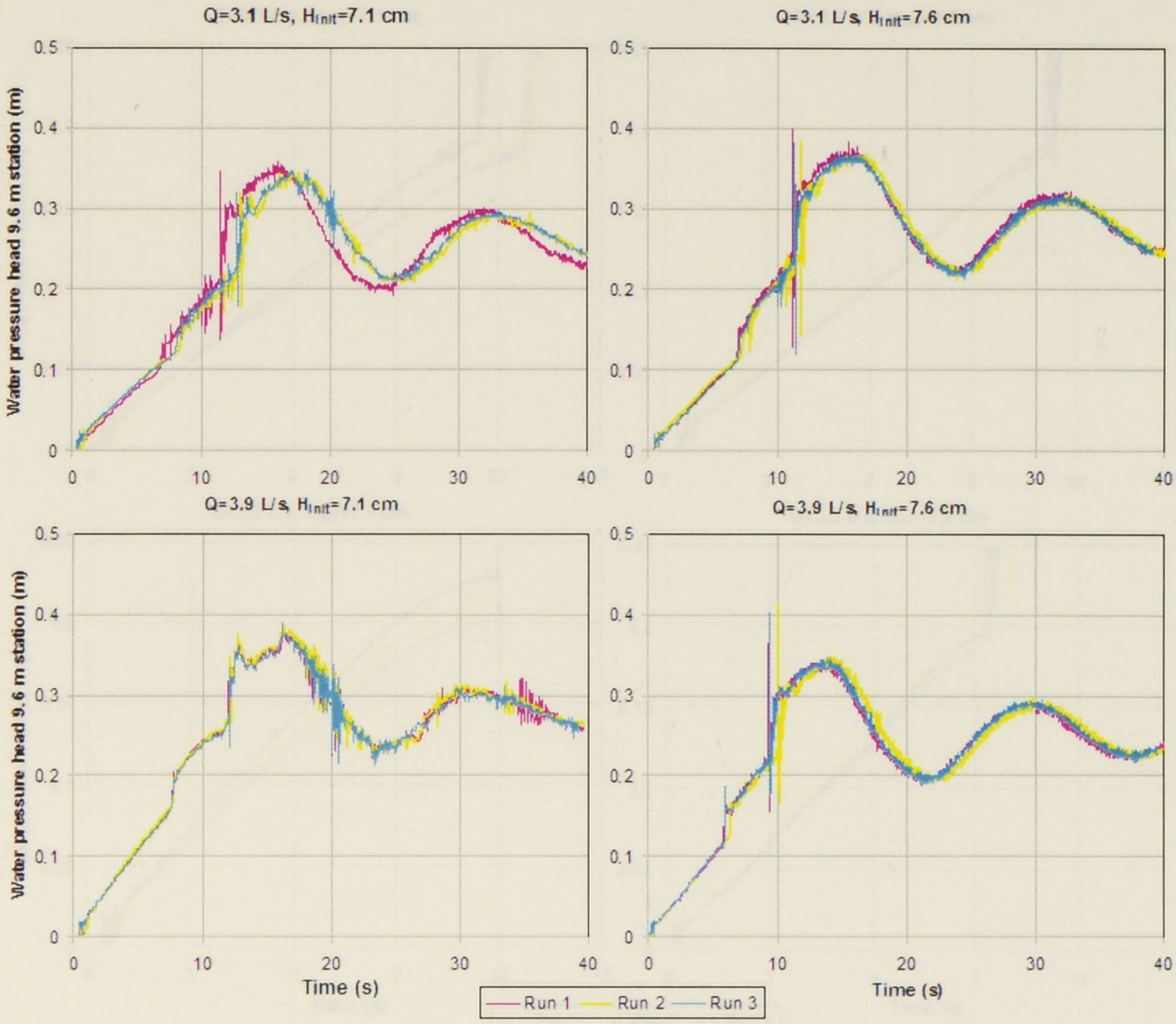

Figure 5.4: Water pressure at the 9.6 m station for different settings of phase three experiments

The results of the water pressure head at the 9.6 m station for all the experimental settings are shown in figure 5.4. As expected, there's in immediate increase in the pressure caused by the air pressurization. A jump in the pressure observed between T=5 s and T=10 s is caused by the passage of the pressurization bore. There are some discrepancies in the results of setting A, and this is because the one of the repetitions had a slighly higher initial water level. The pressure spikes detected in some runs after the bore arrived at the surge tank are related to sudden air releases in the system. The oscillations in the pressure are result of the surges oscillations on the riser.

The results from the air pressure measurements promoted with the transducers located on the top of the pipe at the 14.1 m station are shown in figure 5.5. The results demonstrate sn immediate increase of the air pressure as the flow is initiated. The "air-cushioning" effect retarding the bore arrival at the riser is evident.

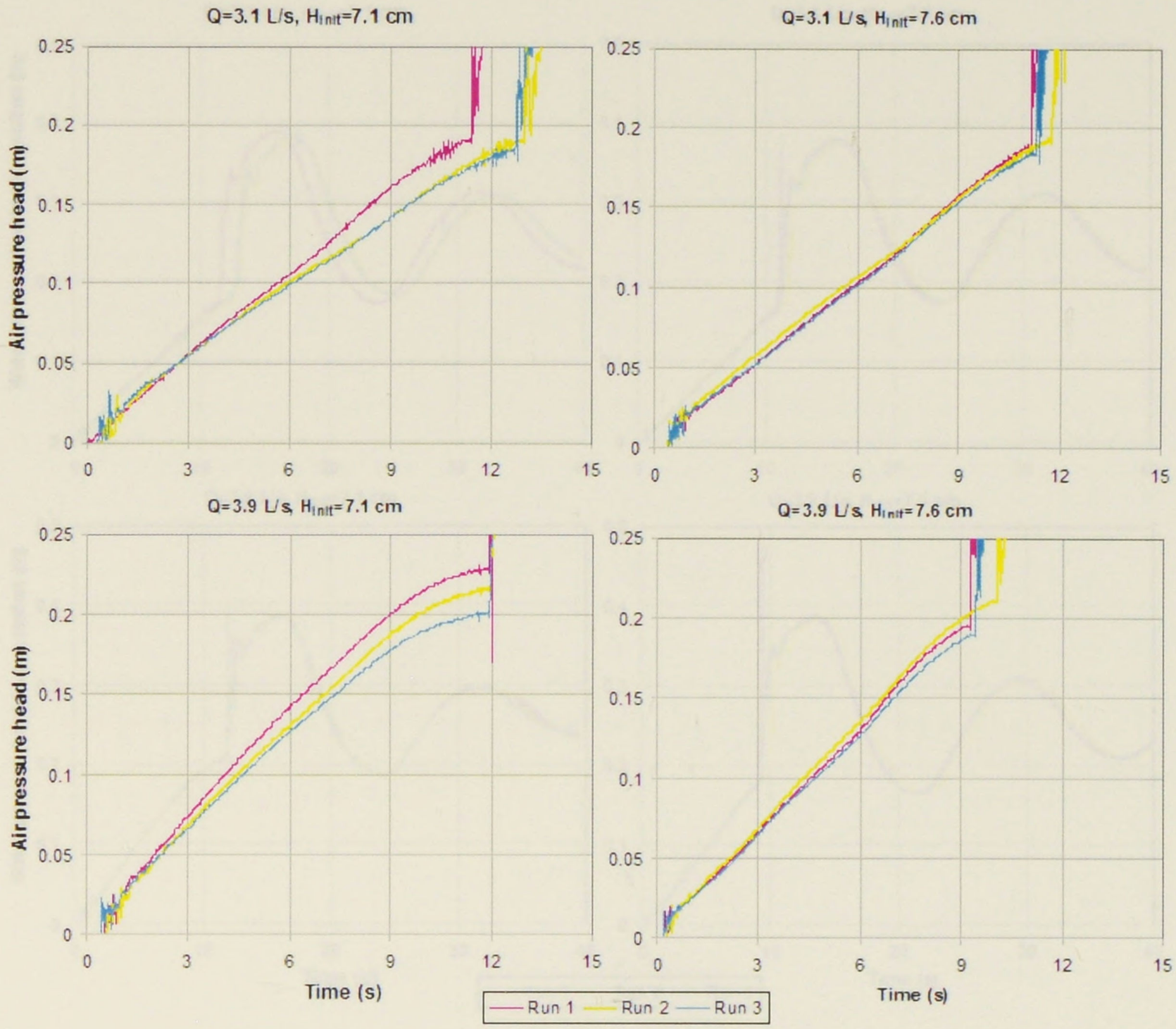

Figure 5.5: Air pressure head at the 14.1 m station for different settings of phase three experiments

The discrepancy in the results of setting A due to the higher initial water level is also noticed here. This transducer is the only one located at the top of the pipe, experiencing thus phase change during the runs. That can be the explanation for the discrepancies observed in the results from the repetitions of setting C.

The measurements of the water pressure head at the 14.1 m station are shown in figure 5.6, and there's good consistency between the repetitions. The only apparent problem with one of the runs of setting A is again due to the slightly higher initial water level in one of the repetitions. Most of the observations made for the 9.6 m station are also applicable here.

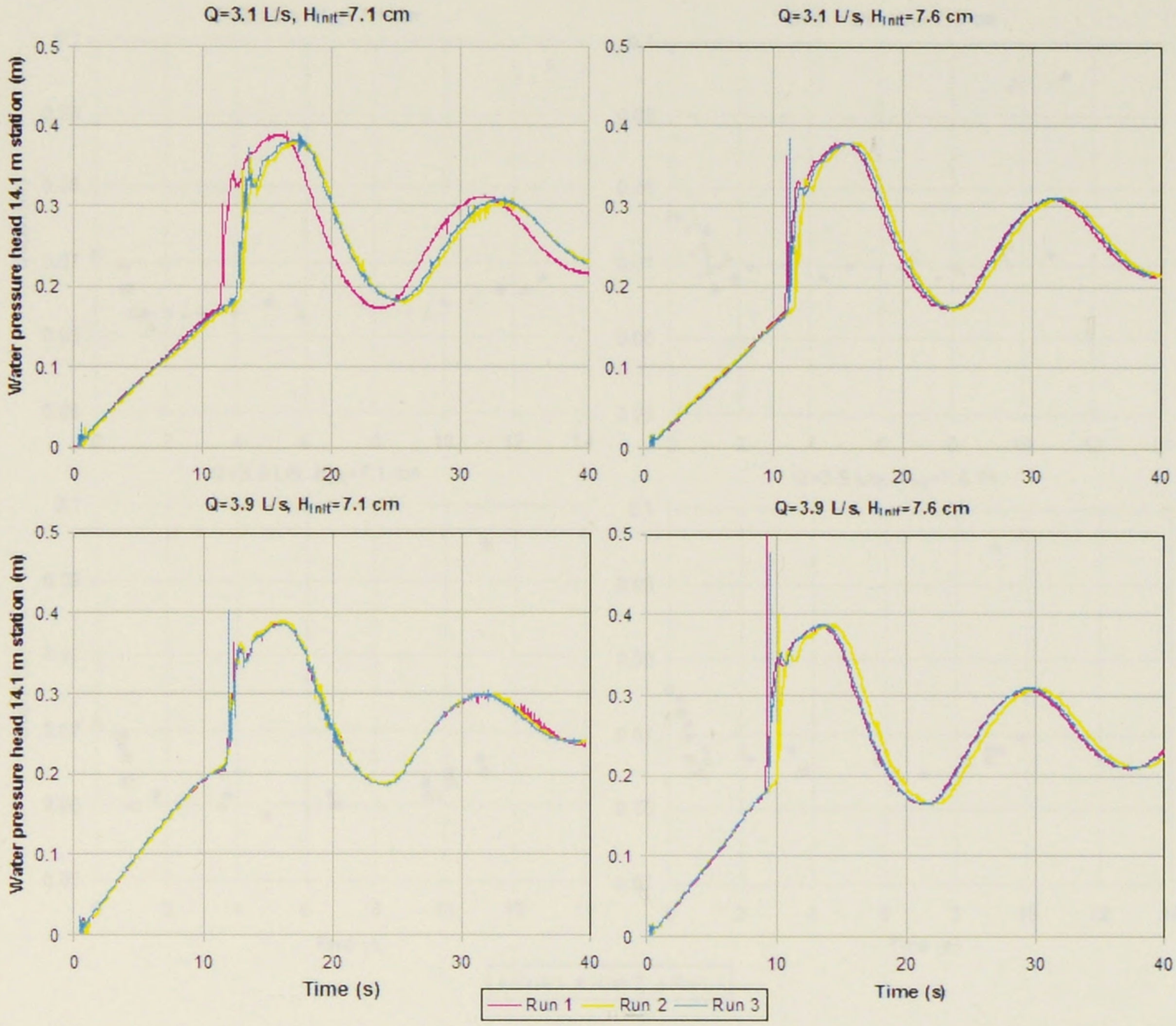

Figure 5.6: Water pressure at the 14.1 m station for different settings of phase three experiments

The results of the depth measurements promoted at the 14.1 m show generally a good consistency between the repetitions. The results show an almost instantaneous decrease on the water level resulting from the air pressurization. The water level increases again only when the pressurization bore arrives at that station. There are small deviations in the depth measurements that can be explained by small ripples formed on the water surface caused by the relative motion of the air phase. The discrepancies in the bore arrival times observed can be explained in part by imprecisions on the start-up of that particular experimental run, causing the arrival of the bore to arrive at a slightly different time.

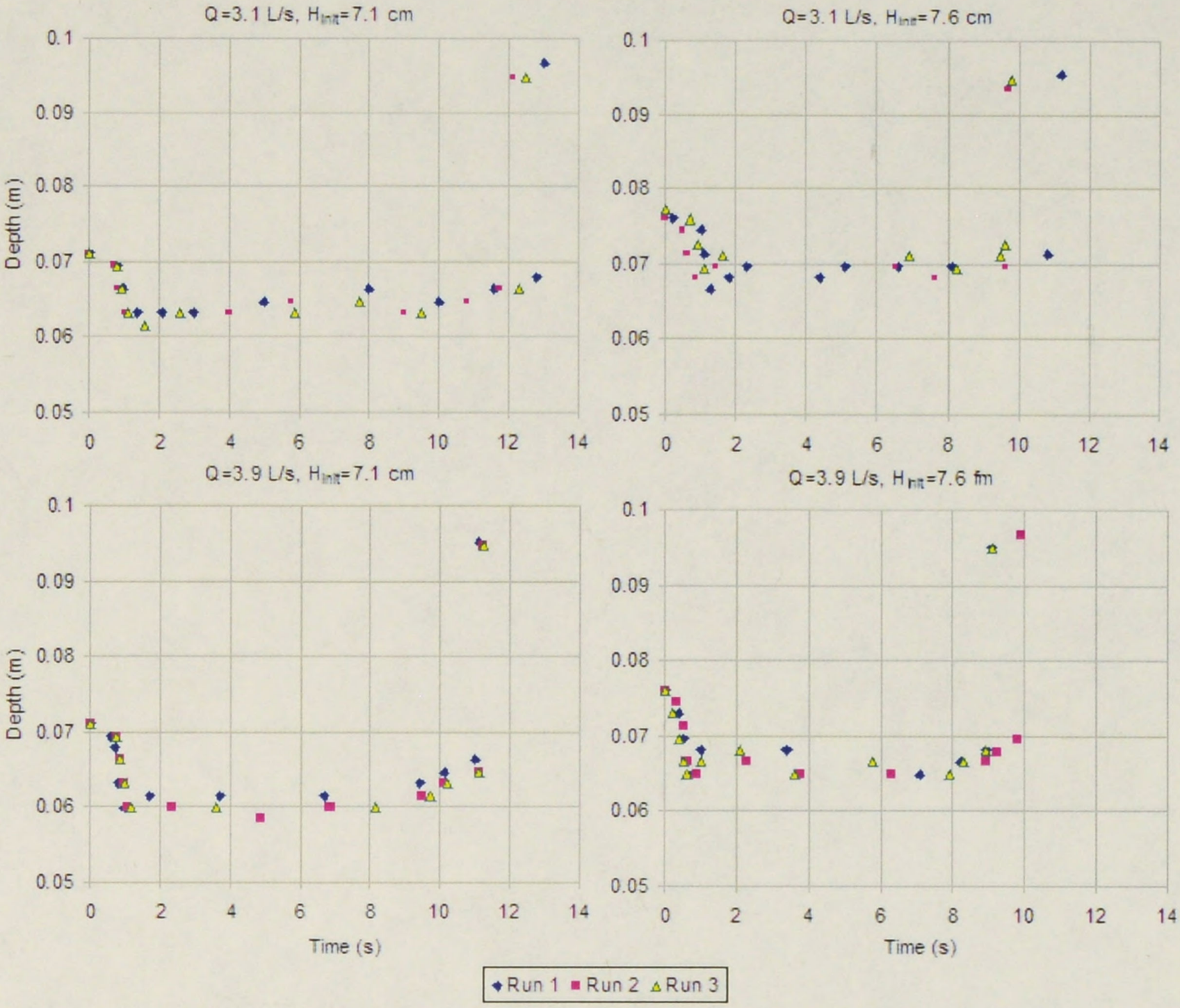

Figure 5.7: Depth measurements at the 14.1 m station for different settings of phase three experiments

5.2 Modeling the rapid filling pipe problem

Many numerical modeling investigations of flow regime transitions and the rapid filling pipe problem have been promoted in the past 3 decades. Among the initial models, one includes works by Wiggert (1972), Cunge et al. (1980), Song et al. (1983), among others, providing different model approaches to the description of the problem.

There are particular difficulties to model this problem arising from differences in the characteristics of free-surface and pressurized flow regimes. First, the celerity of free-surface flows can be between two to three orders of magnitude smaller than the correspondent one for pressurized flow. Second, while pressurized flow can occur with negative gage pressures, such is not possible in the free-surface flow regime. Third, with multiple inflow points, the possibility exists for multiple

flow regime transitions to occur simultaneously. Finally, the calculation of the pressurization bore requires the conservation of mass and momentum across it, and the sharp discontinuity in the depth across the bore may pose difficulties in terms of the numerical scheme to be used (Glaister, 1988).

There are also model difficulties related to the presence of the air phase inside tunnels during the rapid filling pipe event. The first one is to choose between a single-phase model approach, in which only the mass and momentum equations for the water phase are used, or a two-phase flow model, in which mass and momentum equations for both phases are used. The second is to determine which numerical scheme is to be used in the solution of the problem. Finally it must be decided which interactions between phases must be handled by the model. A detailed discussion regarding these difficulties is provided in Vasconcelos and Wright (2005).

One can generally classify the different numerical models for the rapid filling pipe problem in two basic groups: interface-tracking models and Preissmann-slot based models. Interface-tracking models apply different sets of equations to the description of the pressurized and free-surface portions of the flow, requiring the computation of the pressurization front location at each time step. In contrast, the models using the Preissmann-slot concept apply the Saint-Venant equations throughout the domain. These type of models introduce a hypothetical, narrow slot at the top of the sewers, which emulates the surcharge in the sewers while allowing the problem to be calculated by free surface flow equations.

5.2.1 Modeling the water phase

The model used is presented in the work by Vasconcelos and Wright (2005), and is a one-dimensional, single-phase model, based on the Preissmann slot concept. The model solves the Saint-Venant equations, modified to incorporate the effects of the air phase pressurization:

$$\frac{\partial \vec{U}}{\partial t} + \frac{\partial \vec{F}}{\partial x} = \vec{S}$$

For a location without air phase

$$\vec{U} = \begin{bmatrix} A \\ Q \end{bmatrix}, \vec{F} = \begin{bmatrix} Q \\ \frac{Q^2}{A} + gI \end{bmatrix}$$
$$\vec{S} = \begin{bmatrix} 0 \\ gA(S_o - S_f) \end{bmatrix} \tag{5.1}$$

For a location with air phase

$$\vec{U} = \begin{bmatrix} A \\ Q \end{bmatrix}, \vec{F} = \begin{bmatrix} Q \\ \frac{Q^2}{A} + gI + gAH_{air} \end{bmatrix}$$
$$\vec{S} = \begin{bmatrix} 0 \\ gA(S_o - S_f) + \frac{1}{\rho_w} F_i B \end{bmatrix}$$

In which: A is cross sectional area of water flow, Q is the water flow rate, I is the 1st moment of the cross sectional area about the free surface, H_{air} is the air phase pressure head, S_o is the bed slope, S_f is the energy slope (given by Manning equation), ρ_w is the water density (assumed constant), B is the free surface width, F_i is the shear forces between the phases.

The possibility of discontinuities (bores) in the solution characterizes the rapid filling as a Riemann initial value problem. According to Godunov's theorem, numerical models based on linear schemes yield either numerical diffusion of the front or unrealistic numerical oscillations in the vicinity of discontinuities . Thus, one need to avoid the use of linear schemes such as the Lax-Friedrich scheme or the Lax-Wendroff scheme. One alternative is to apply an approximate Riemann solver such as the one proposed by Roe (1981).

To compute the updated values of A and Q using Roe's scheme, one needs to solve the Riemann problem approximately in each one of the finite cell interfaces. That requires the calculation of the fluxes on each side of the interfaces as well the contribution of the wave that intersects the control volume. Following Macchione and Morelli (2003), the updated value for the quantitites $\vec{U}$ are provided by:

$$\begin{aligned}\vec{U}^{n+1} = \vec{U}^n - \frac{\Delta t}{2\Delta x}\left[(\vec{F}^n_{i+1} + \vec{F}^n_i) - \sum_j |\lambda^{(j)}|(\delta w^{(j)})_{i+1/2}\bar{r}^{(j)}_{i+1/2}\right] \\ + \frac{\Delta t}{2\Delta x}\left[(\vec{F}^n_{i-1} + \vec{F}^n_i) - \sum_j |\lambda^{(j)}|(\delta w^{(j)})_{i-1/2}\bar{r}^{(j)}_{i-1/2}\right] + \Delta t \vec{S}^n_i\end{aligned} \tag{5.2}$$

In the above equation, n is the time index. The values of the approximate values of the eigenvalues $\lambda^{(j)}$ and the correspondent eigenvectors $\bar{r}^{(j)}$ for A and Q across the interface require first the computation of the so-called Roe averages across each one of the interfaces (i, i+1).

$$\bar{A}_{i+1/2} = \sqrt{A_{i+1}A_i} \tag{5.3a}$$

$$\bar{Q}_{i+1/2} = \frac{\sqrt{A_{i+1}}\,Q_i + \sqrt{A_i}\,Q_{i+1}}{\sqrt{A_{i+1}} + \sqrt{A_i}} \tag{5.3b}$$

$$\bar{c}_{i+1/2} = \sqrt{g\frac{I_{i+1} - I_i}{A_{i+1} - A_i}} \quad \text{if} \quad A_{i+1} \neq A_i \tag{5.3c}$$

$$\bar{c}_{i+1/2} = \sqrt{g\frac{1/2(A_{i+1} + A_i)}{1/2(B_{i+1} + B_i)}} \text{ if } A_{i+1} = A_i \tag{5.3d}$$

in which: B is the width of the free surface.

With these values calculated, we now obtain the approximate eigenvalues and eigenvectors across interfaces (i,i+1) with the equations:

$$\bar{\lambda}^{(1)} = \frac{\bar{Q}}{\bar{A}} + \bar{c} \tag{5.4a}$$

$$\bar{\lambda}^{(2)} = \frac{\bar{Q}}{\bar{A}} - \bar{c} \tag{5.4b}$$

$$\bar{r}^{(1)} = \frac{1}{2\bar{c}}\begin{bmatrix}1 & \bar{\lambda}^{(1)}\end{bmatrix}^T \tag{5.4c}$$

$$\bar{r}^{(2)} = \frac{1}{2\bar{c}}\begin{bmatrix}1 & \bar{\lambda}^{(2)}\end{bmatrix}^T \tag{5.4d}$$

Finally, the strength of the wave crossing the cell, measured in terms of the variations δw at the interface, can be obtained with the equations:

$$\delta w^{(1)(2)} = \pm\Big[(Q_{i+1} + Q_i) + \Big(-\frac{\bar{Q}_{i+1/2}}{\bar{A}_{i+1/2}} \pm \bar{c}_{i+1/2}\Big)(A_{i+1} - A_1)\Big] \tag{5.5}$$

This set of equations must be solved for all internal finite volume cells within each time step. The system boundaries are comprised of an inflow box at the upstream end and a surge tank at the downstream end. At the upstream end the unknowns are the discharge entering the 1st cell, the flow area at the 1st cell and the water level in the fill box. There are three equations available: the C- characteristic equation, obtained with data from cells 1 and 2 from the previous time step; the energy equation between the fill box and the 1st cell; and the continuity equation. That set of equations needs to be solved iteratively until convergence. Similarly, at the downstream end, the unknowns are the discharge and flow area at the last cell, and the water level at the surge tank. The equations used now to solve are the y-momentum equation in the surge tank (thus accounting for the inertia in the surge tank), C+ characteristic equation and continuity. An iterative process is also used here to achieve convergence.

5.2.2 Modeling the air phase

In order to avoid the difficulties of dealing with two-phase flow models, some simplifications are required to the description of the air phase flow inside of the system. These simplifications transform the partial differential equations describing the mass and momentum balance into simple algebraic expressions. These simplifications may prevent a more accurate description of the interactions between the phases. However, the difficulties to implement a two-phase Riemann solver using the four pde's and adapted to the characteristics of this problem have not been overcome yet. In any case, for the purposes of this work, the simplified approach to describe the air phase proved to be sufficiently precise.

The first simplification is with regards to the air phase continuity equation. The wave celerity in the air phase is much faster than the speed of the superficial disturbances in the free surface region or than the speed of the pressurization bore. Thus, one may assume air phase flow as quasi-steady since there's enough time for several reflections of the air pressure transients within the discretized domain for each discrete advance of the pressurization bore. That assumption allows for an important simplification of the mass balance equation for the air phase (eq. 5.6):

$$\frac{dM}{dt} = 0 \tag{5.6}$$

in which: M is the air mass rate of flow and t is time.

As a result, the continuity equation for the air phase written in the discretized domain becomes:

$$\rho_i A_i V_i = \rho_{i-1} A_{i-1} V_{i-1} \tag{5.7}$$

in which: i is the grid cell index, ρ is the air density, A is the cross sectional area of the air phase and V is the air phase velocity.

Further simplifications are introduced in the air phase momentum equation. Initially, if the flow is quasi-steady, then the temporal derivative disappears from the equation. Because the problem

deals with quasi-horizontal conduits, the gravity terms are dropped from the equation as well. The only terms left are related to the pressure gradient and frictional forces. Following the development provided in Wylie and Streeter (1993) for steady state equations in gas pipelines, we have the equation that relates the air pressure between two points in the pipeline:

$$p_i^2 = p_{i-1}^2 - \frac{f c_a^2 M^2}{DA^2} \Delta x \tag{5.8}$$

in which: p is the air pressure, f is the friction factor (assumed constant), c_a is acoustic wavespeed in the air, D is the effective diameter, and Δx is the distance between grid cell centerpoints.

Finally, to achieve closure of the equations that describe the air phase pressure, we need to define a relationship between air density and pressure. This model assumes that air phase will undergo an isothermal compression, so

$$\sqrt{\frac{p}{\rho}} = c_a = constant \tag{5.9}$$

The boundary conditions for the air phase are calculated in the following manner. At each time step, the net volume of water that has entered the tunnel equals the volume of air that has left the system. Because air density changes between each time step, a simple orifice equation is used to relate the air discharge with the pressure head at the discharge point, based on Zhou et al. (2002):

$$Q_{air} = C_d A_{orif} \sqrt{2g \frac{\rho_w}{\rho_a} H_{air}} \tag{5.10}$$

in which: Q_{air} is the volumetric flow rate of air, C_d is the orifice discharge coefficient, A_{orif} is the available ventilation area, g is gravity, ρ_a is the density of the air phase at the discharge point and H_{air} is the air phase pressure head.

The calculation follows this procedure: given the net water flow entering the tunnel Q_w, the value for Q_{air} is obtained by setting $Q_{air} = Q_w$. At the discharge point, the value for H_{air} is obtained using equation 5.10, allowing for the calculation of the new values for p and ρ_a at the discharge point. The value of the air phase mass flow M (assumed steady) is obtained by setting $M = Q_{air}\rho_{air}$ at the discharge point. To determine the air phase density, pressure and velocity for all cells upstream from the discharge point, equations 5.7, 5.8 and 5.9 are used. Calculations stop in the section where the pressurization bore is located.

5.2.3 Numerical predictions of the IBD occurrence

The results of the numerical prediction of the IBD for setting A of phase three experiments is shown in figure 5.8.

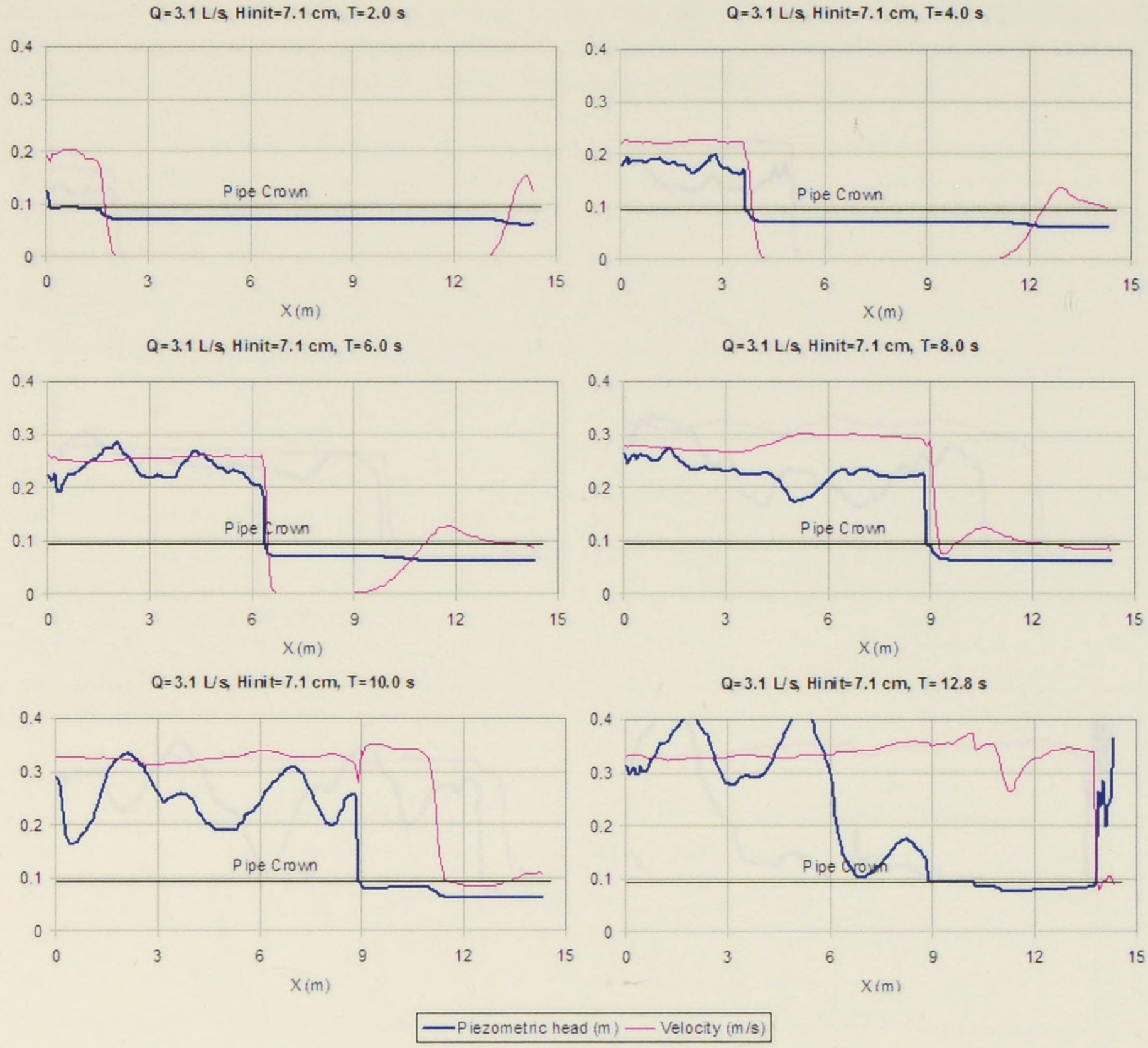

Figure 5.8: Numeric predictions of the depth and velocity profiles for different times. Q=3.1 L/s and H_{init}=7.1 cm

The first snapshot illustrates the bore almost filling the cross section when T=2 s. The "pre-bore motion" feature is also formed at the downstream end. At T=4 s the pipe-filling bore is already at 25% of the pipe length with the "pre-bore motion" noticeable at x=11 m. The two flow features meet at T=8 s, and the onset of the IBD is noticeable. As times advances, the air pocket continues to expand, until it's trapped at T=12.8 s. While the numerical predictions of the IBD suggests the occurence at x=9 m, visual observations indicates the location of occurrence as x=9.3 m. This is considered a very good agreement between the model and the experimental results.

The results of the numerical prediction of the IBD for setting B of phase three experiments is shown in figure 5.9.

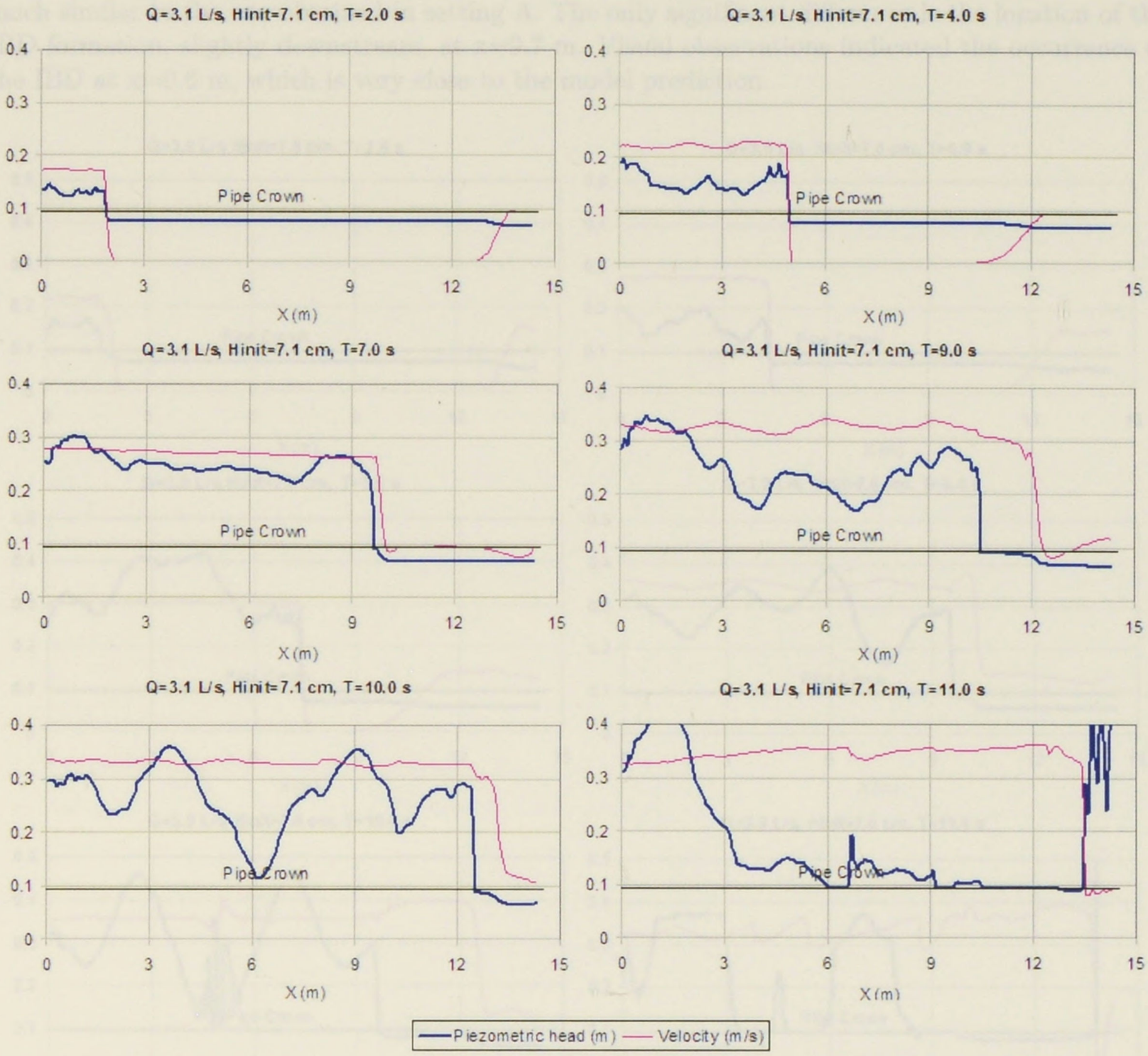

Figure 5.9: Numeric predictions of the depth and velocity profiles for different times. Q=3.1 L/s and H_{init}=7.6 cm

This is a case in which the visual observations pointed to the IBD occurrence, followed by the reformation of the pipe-filling bore. As a result, the air pocket trapped within the pipe in this setting was much smaller than the one in setting A. The numerical prediction shows that the pipe-filling bore and the "pre-bore motion" features meet at T=7 s, followed by the onset of the IBD. However, unlike setting A predictions, the air wedge is pushed downstream and follows the bore, which doesn't close the pipe cross section. The bore is practically reformed at T=10 s, and when the bore arrives at the surge tank at T=11 s, the air pocket entrapped is much smaller than the pocket formed in setting A. Again, the numerical prediction is in good agreement with the experimental results.

The numerical prediction of the IBD formation for setting C, depicted in figure 5.10, is very

much similar to the one obtained in setting A. The only significant difference is the location of the IBD formation, slightly downstream, at x=9.7 m. Visual observations indicated the occurrence of the IBD at x=9.6 m, which is very close to the model prediction.

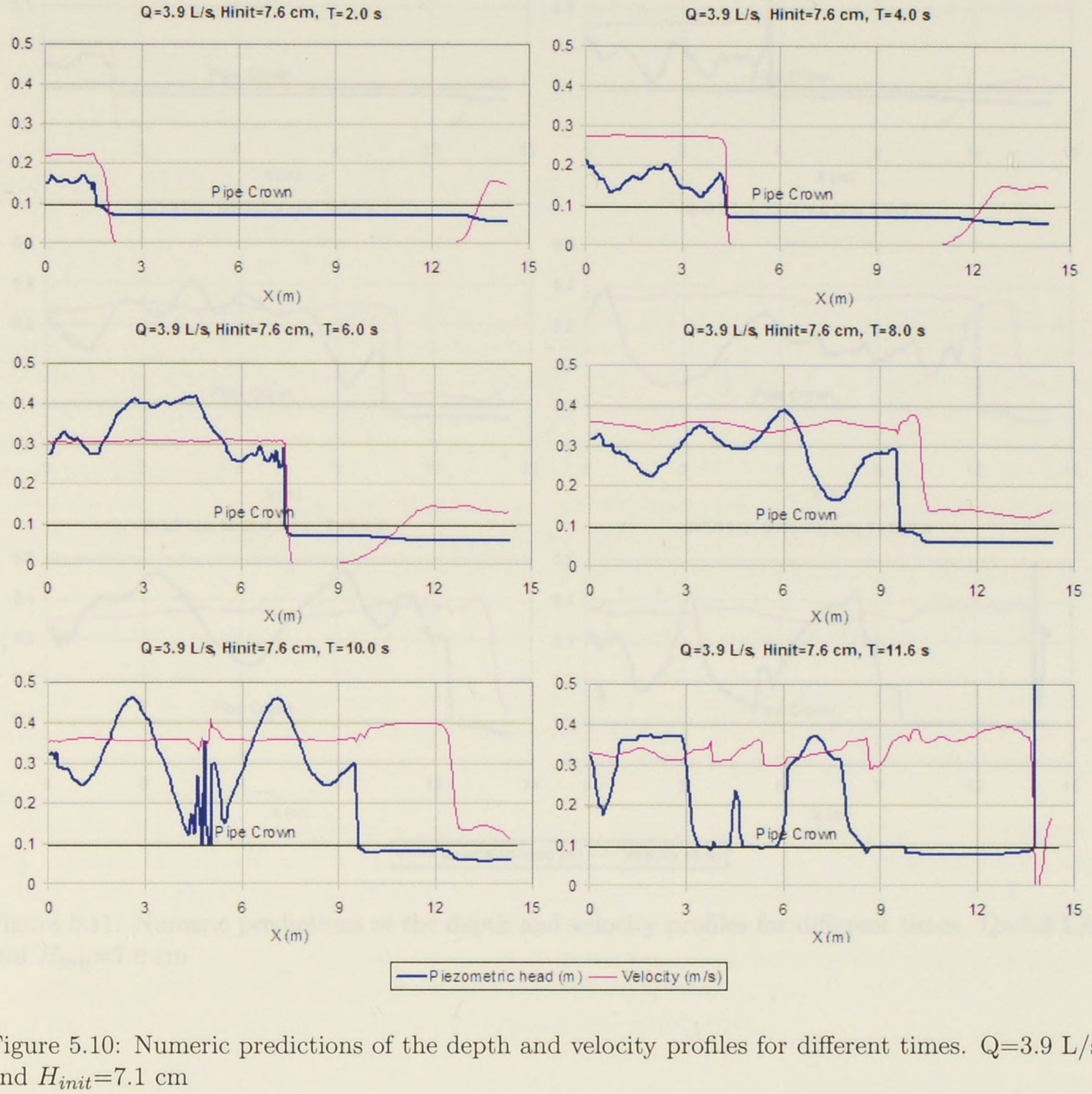

Figure 5.10: Numeric predictions of the depth and velocity profiles for different times. Q=3.9 L/s and H_{init}=7.1 cm

Finally, the results of the numerical prediction of the IBD for setting D of phase three experiments is shown in figure 5.11. As in the setting B predictions, there's the IBD occurrence at T=7 s, but the air intrusion is pushed downstream towards the vent point by the pressurization front. The pipe-filling bore is almost totally reformed at T=9 s, and when the bore arrives at the surge tank the air pocket entrapped is much smaller than the correspondent one from setting C.

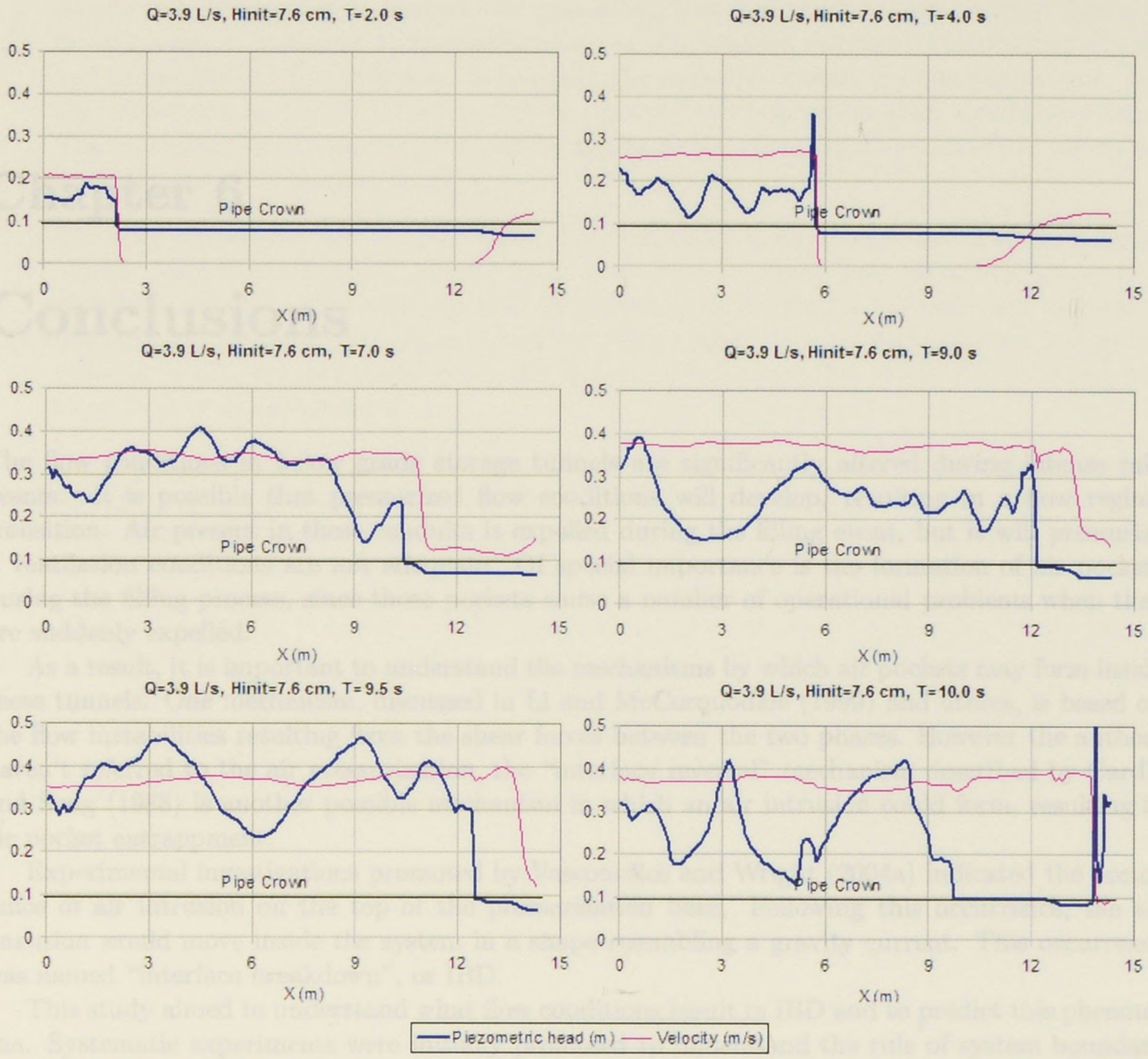

Figure 5.11: Numeric predictions of the depth and velocity profiles for different times. Q=3.9 L/s and H_{init}=7.6 cm

Chapter 6

Conclusions

The flow conditions in below grade storage tunnels are significantly altered during intense rain events. It is possible that pressurized flow conditions will develop, resulting in a flow regime transition. Air present in these conduits is expelled during the filling event, but it will pressurize if ventilation conditions are not adequate. Of special importance is the formation of air pockets during the filling process, since those pockets cause a number of operational problems when they are suddenly expelled.

As a result, it is important to understand the mechanisms by which air pockets may form inside these tunnels. One mechanism, discussed in Li and McCorquodale (1999) and others, is based on the flow instabilities resulting from the shear forces between the two phases. However the authors haven't referred to the air pressurization, the "interface reversal" mechanism described by Cardle and Song (1988) is another possible mechanism in which an air intrusion could form, resulting in air pocket entrappment.

Experimental investigations promoted by Vasconcelos and Wright (2004a) indicated the occurrence of air intrusion on the top of the pressurization bore. Following this occurrence, the air intrusion would move inside the system in a shape resembling a gravity current. This occurrence was named "interface breakdown", or IBD.

This study aimed to understand what flow conditions result in IBD and to predict this phenomena. Systematic experiments were initially promoted to understand the rule of system boundary geometry in the phenomena occurrence. In sequence, further experiments aimed to detail flow conditions on the vicinity of the pressurization bore using pressure transducers at the vicinity of the IBD occurrence. Finally, a restricted set of experiments was promoted to gather data to construct a numerical model that was aimed to predict the IBD occurrence.

The conclusions from this study can be summarized as following:

- Events on the system boundaries have no impact on the IBD occurrence. It was initially hipothesized that the spilling at the fill box or the level stabilization at the riser could trigger IBD. It was demonstrated however that IBD wasn't related to such events. The geometry of the fill box, however, has an effect on whether the pipe-filling bore will form or not.

- There are cases in which the air intrusion caused by IBD is eliminated due to the advance of the pressurization bore, resulting in the pipe-filling bore reformation;

- The mechanism of the IBD occurrence is related to the flow conditions at the bore vicinity,

specifically the interaction between the pipe-filling bore and the "pre-bore motion" features. In this sense, it is similar to the mechanisms of the "iterface reversal" described by Cardle and Song (1988). The difference is basically the causative factors for the phenomena, and the subsequent motion of the air pocket as a gravity current, rather than a retreating front. The pipe-filling bore reformation would be similar to the change of direction of the retreating interface described by that study;

- The IBD occurrence and the pipe-filling bore reformation were both described by a Saint-Venant equations numerical solver, which accounted for the effects of the air phase in a simplified manner. This code was able to predict with reasonable accuracy the location of the IBD. But because this numeric approach is a single-phase model, it cannot model the behavior of air pockets formed within the system. A two-phase flow model would be required to perform such calculations;

- Further experimental studies are also required to determine the amount of ventilation and its distribution within storage tunnels so that IBD and other undesired conditions related to air pressurization can be avoided.

Bibliography

Cardle, J. A. and Song, C. S. S. (1988). "Mathematical modeling of unsteady flow in storm sewers." *Int. J. Engrg. Fluid Mech.*, 1(4), 495–518.

Cunge, J. A., Jr., F. M. H., and Verwey, A. (1980). *Practical Aspects of Computational River Hydraulics.* Pitman Publishing Ltd., London, UK.

Glaister, P. (1988). "Approximate riemann solutions of the shallow water equations." *J. Hydr. Res.*, 26(3), 293–306.

Guo, Q. and Song, C. S. S. (1990). "Surging in urban storm drainage systems." *J. Hydr. Engrg.*, 116(12), 1523–1537.

Guo, Q. and Song, C. S. S. (1991). "Dropshaft hydrodynamics under transient conditions." *J. Hydr. Engrg.*, 117(8), 1042–1055.

Hager, W. H. (2001). "Swiss contribution to water hammer theory." *J. Hydr. Res.*, 39(1), 3–10.

Hamam, M. A. and McCorquodale, J. A. (1982). "Modeling mixed flow in storm sewers." *Ca. J. Civ. Engrg.*, (9), 189–196.

Li, J. and McCorquodale, A. (1999). "Modeling mixed flow in storm sewers." *J. Hydr. Engrg.*, 125(11), 1170–1180.

Macchione, F. and Morelli, M. A. (2003). "Practical aspects in comparing the shock-capturing schemes for dam break problems." *J. Hydr. Engrg.*, 129(3), 187–195.

Nguyen, T. D. (1999). "Numerical simulation of the flow in a conduit in the presence of a confined air cushion." *Int. J. Num. Meth. in Fluids*, 29(4), 485–498.

Roe, P. L. (1981). "Approximate riemann solvers, parameter vectors, and difference schemes." *J. Comp. Physics*, 43, 357–372.

Song, C. S. S., Cardle, J. A., and Leung, K. S. (1983). "Transient mixed-flow models for storm sewers." *J. Hydr. Engrg.*, 109(11), 1487–1504.

Vasconcelos, J. G. and Wright, S. J. (2004a). "Experimental investigation of large surges generated in stormwater storage tunnels with restricted venting conditions. Submitted to the Journal of Hydraulic Engineering.

Vasconcelos, J. G. and Wright, S. J. (2004b). "Numerical modeling of the transition between free surface and pressurized flow in storm sewers." *Innovative Modeling of Urban Water Systems, Monograph 12*, W. James, ed., CHI Publications, Ontario, Canada.

Vasconcelos, J. G. and Wright, S. J. (2005). "Applications and limitations of single-phase models to the description of the rapid filling pipe problem." *Conf. Stormwater and Urban Water Systems Modeling*, W. James, ed., Ontario, Canada. CHI Publications.

Wiggert, D. C. (1972). "Transient flow in free-surface, pressurized systems." *J. Hydr. Div.*, 98(HY1), 11–27.

Wright, S. J., Vasconcelos, J. G., and Ridgway, K. (2003). "Surges associated with filling of stormwater storage tunnels." *Practical Modeling of Urban Water Systems, Monograph 11*, W. James, ed., CHI Publications, Ontario, Canada.

Wylie, E. B. and Streeter, V. L. (1993). *Fluid Transients in Systems.* Prentice Hall, Upper Saddle River, NJ.

Zhou, F., Hicks, F. E., and Steffler, P. M. (2002). "Transient flow in a rapidly filling horizontal pipe containing trapped air." *J. Hydr. Engrg.*, 128(6), 625–634.

Zoppou, C. (1999). "Review of stormwater models." *Report No. 52/99*, CSIRO Land and Water, Canberra, Australia.

AIIM SCANNER TEST CHART # 2

Spectra

4 PT ABCDEFGHIJKLMNOPQRSTUVWXYZabcdefghijklmnopqrstuvwxyz:'',./?$0123456789

6 PT ABCDEFGHIJKLMNOPQRSTUVWXYZabcdefghijklmnopqrstuvwxyz;:'',./?$0123456789

8 PT ABCDEFGHIJKLMNOPQRSTUVWXYZabcdefghijklmnopqrstuvwxyz;:'',./?$0123456789

10 PT ABCDEFGHIJKLMNOPQRSTUVWXYZabcdefghijklmnopqrstuvwxyz;:'',./?$0123456789

Times Roman

4 PT ABCDEFGHIJKLMNOPQRSTUVWXYZabcdefghijklmnopqrstuvwxyz;:'',./?$0123456789

6 PT ABCDEFGHIJKLMNOPQRSTUVWXYZabcdefghijklmnopqrstuvwxyz;:'',./?$0123456789

8 PT ABCDEFGHIJKLMNOPQRSTUVWXYZabcdefghijklmnopqrstuvwxyz;:'',./?$0123456789

10 PT ABCDEFGHIJKLMNOPQRSTUVWXYZabcdefghijklmnopqrstuvwxyz;:'',./?$0123456789

Century Schoolbook Bold

4 PT **ABCDEFGHIJKLMNOPQRSTUVWXYZabcdefghijklmnopqrstuvwxyz;:'',./?$0123456789**

6 PT **ABCDEFGHIJKLMNOPQRSTUVWXYZabcdefghijklmnopqrstuvwxyz;:'',./?$0123456789**

8 PT **ABCDEFGHIJKLMNOPQRSTUVWXYZabcdefghijklmnopqrstuvwxyz;:'',./?$0123456789**

10 PT **ABCDEFGHIJKLMNOPQRSTUVWXYZabcdefghijklmnopqrstuvwxyz;:'',./?$0123456789**

News Gothic Bold Reversed

4 PT ABCDEFGHIJKLMNOPQRSTUVWXYZabcdefghijklmnopqrstuvwxyz;:'',./?$0123456789

6 PT ABCDEFGHIJKLMNOPQRSTUVWXYZabcdefghijklmnopqrstuvwxyz;:'',./?$0123456789

8 PT ABCDEFGHIJKLMNOPQRSTUVWXYZabcdefghijklmnopqrstuvwxyz;:'',./?$0123456789

10 PT ABCDEFGHIJKLMNOPQRSTUVWXYZabcdefghijklmnopqrstuvwxyz;:'',./?$0123456789

Bodoni Italic

4 PT ABCDEFGHIJKLMNOPQRSTUVWXYZabcdefghijklmnopqrstuvwxyz;:'',./?$0123456789

6 PT ABCDEFGHIJKLMNOPQRSTUVWXYZabcdefghijklmnopqrstuvwxyz;:'',./?$0123456789

8 PT ABCDEFGHIJKLMNOPQRSTUVWXYZabcdefghijklmnopqrstuvwxyz;:'',./?$0123456789

10 PT ABCDEFGHIJKLMNOPQRSTUVWXYZabcdefghijklmnopqrstuvwxyz;:'',./?$0123456789

Greek and Math Symbols

4 PT ΑΒΓΔΕΞΘΗΙΚΛΜΝΟΠΦΡΣΤΥΩΧΨΖαβγδεξθηικλμνοπφρστυωχψζ≧∓'',. / ≦±=≠°><⊁⊀⩾⩽≡

6 PT ΑΒΓΔΕΞΘΗΙΚΛΜΝΟΠΦΡΣΤΥΩΧΨΖαβγδεξθηικλμνοπφρστυωχψζ≧∓'',. / ≦±=≠°><⊁⊀⩾⩽≡

8 PT ΑΒΓΔΕΞΘΗΙΚΛΜΝΟΠΦΡΣΤΥΩΧΨΖαβγδεξθηικλμνοπφρστυωχψζ≧∓'',. / ≦±=≠°><⊁⊀⩾⩽≡

10 PT ΑΒΓΔΕΞΘΗΙΚΛΜΝΟΠΦΡΣΤΥΩΧΨΖαβγδεξθηικλμνοπφρστυωχψζ≧∓'',. / ≦±=≠°><⊁⊀⩾⩽≡

White

Black

Isolated Characters

e	m	1	2	3	a
4	5	6	7	o	°
8	9	0	h	I	B

A4 Page 6543210

MESH HALFTONE WEDGES

65

85

100

110

133

150

A4 Page 6543210

RIT ALPHANUMERIC RESOLUTION TEST OBJECT, RT-1-71

PRODUCED BY GRAPHIC ARTS RESEARCH CENTER

ROCHESTER INSTITUTE OF TECHNOLOGY, ONE LOMB

MEMORIAL DRIVE, ROCHESTER, NEW YORK 14623